bioRxiv preprint doi: https://doi.org/10.1101/063271; this version posted October 22, 2016. The copyright holder for this preprint (which was not certified by peer review) is the author/funder. All rights reserved. No reuse allowed without permission.

1 **Benzoate and Salicylate Tolerant Strains Lose Antibiotic Resistance during Laboratory**
2 **Evolution of *Escherichia coli* K-12**
3
4 by
5 Kaitlin E. Creamer,[1*] Frederick S. Ditmars,[1*] Preston J. Basting,[1*]
6 Karina S. Kunka,[1] Issam N. Hamdallah,[1] Sean P. Bush,[1] Zachary Scott,[1] Amanda He,[1]
7 Stephanie R. Penix,[1] Alexandra S. Gonzales,[1] Elizabeth K. Eder,[1] Dominic Camperchioli,[1]
8 Adama Berndt,[1] Michelle W. Clark,[1] Kerry A. Rouhier,[2] and Joan L. Slonczewski[1]
9
10 **Corresponding Author:**
11 Joan L. Slonczewski
12 Robert A. Oden, Jr. Professor of Biology
13 Higley Hall, 202 N. College Road
14 Kenyon College
15 Gambier, OH 43022
16 http://biology.kenyon.edu/slonc/slonc.htm
17 slonczewski@kenyon.edu
18 Phone: 740-427-5397
19
20 **Affiliations:**
21 1. Department of Biology, Kenyon College, Gambier, OH, USA
22 2. Department of Chemistry, Kenyon College, Gambier, OH, USA
23 *These authors contributed equally to the work.

bioRxiv preprint doi: https://doi.org/10.1101/063271; this version posted October 22, 2016. The copyright holder for this preprint (which was not certified by peer review) is the author/funder. All rights reserved. No reuse allowed without permission.

24 ABSTRACT

25 *Escherichia coli* K-12 W3110 grows in the presence of membrane-permeant organic
26 acids that can depress cytoplasmic pH and accumulate in the cytoplasm. We conducted
27 experimental evolution by daily diluting cultures in increasing concentrations of benzoic acid
28 (up to 20 mM) buffered at external pH 6.5, a pH at which permeant acids concentrate in the
29 cytoplasm. By 2,000 generations, clones isolated from evolving populations showed
30 increasing tolerance to benzoate but were sensitive to chloramphenicol and tetracycline.
31 Sixteen clones grew to stationary phase in 20 mM benzoate, whereas the ancestral strain
32 W3110 peaked and declined. Similar growth occurred in 10 mM salicylate. Benzoate-
33 evolved strains grew like W3110 in the absence of benzoate; in media buffered at pH 4.8, pH
34 7.0, or pH 9.0; or in 20 mM acetate or sorbate at pH 6.5. Genomes of 16 strains revealed
35 over 100 mutations including SNPs, large deletions, and insertion knockouts. Most strains
36 acquired deletions in the benzoate-induced multiple antibiotic resistance (Mar) regulon or in
37 associated regulators such as *rob* and *cpxA*, as well as MDR efflux pumps *emrA*, *emrY*, and
38 *mdtA*. Strains also lost or down-regulated the Gad acid fitness regulon. In 5 mM benzoate, or
39 in 2 mM salicylate (2-hydroxybenzoate), most strains showed increased sensitivity to the
40 antibiotics chloramphenicol and tetracycline; some strains were more sensitive than a *marA*
41 knockout. Thus, our benzoate-evolved strains may reveal additional unknown drug resistance
42 components. Benzoate or salicylate selection pressure may cause general loss of MDR genes
43 and regulators.

44

45 IMPORTANCE

bioRxiv preprint doi: https://doi.org/10.1101/063271; this version posted October 22, 2016. The copyright holder for this preprint (which was not certified by peer review) is the author/funder. All rights reserved. No reuse allowed without permission.

46 Benzoate is a common food preservative, and salicylate is the primary active
47 metabolite of aspirin. In the gut microbiome, genetic adaptation to salicylate may involve
48 loss or downregulation of inducible multidrug resistance systems. This discovery implies that
49 aspirin therapy may modulate the human gut microbiome to favor salicylate tolerance at the
50 expense of drug resistance. Similar aspirin-associated loss of drug resistance might occur in
51 bacterial pathogens found in arterial plaques.

bioRxiv preprint doi: https://doi.org/10.1101/063271; this version posted October 22, 2016. The copyright holder for this preprint (which was not certified by peer review) is the author/funder. All rights reserved. No reuse allowed without permission.

52 INTRODUCTION

53 Pathogenic and commensal enteric bacteria maintain cytoplasmic pH homeostasis in
54 the face of extreme external acid (pH 2-4 in the stomach) and the high concentrations of
55 membrane-permeant organic acids in the colon (70-140 mM) (1–6). Many studies have
56 focused on the response and recovery of *E. coli* to external pH stress (1–5), but relatively few
57 studies have focused on the genetic response to membrane-permeant organic acids (permeant
58 acids) (7–9) despite the importance of permeant acids as food preservatives (10). Permeant
59 acids depress cytoplasmic pH, while their anion accumulates in the cytoplasm (5, 7, 11).
60 Some permeant acids also cross the membrane in the unprotonated form, and decrease the
61 proton motive force (PMF); an example is benzoic acid (benzoate), a food preservative found
62 in soft drinks and acidic foods (12). The related molecule salicylic acid (salicylate) is a plant
63 defense regulator (13, 14) as well as the primary active metabolite of acetylsalicylate
64 (aspirin) (15–17). Salicylates enter the human diet from fruits and vegetables, leading to
65 circulating plasma levels as high as 0.1-0.2 μM (18). Furthermore, aspirin therapy for cardio
66 protection and other metabolic conditions (19, 20) may generate plasma levels of 0.2-0.5 mM
67 salicylate (16, 21, 22). Yet despite the important metabolic effects of aspirin, salicylate and
68 benzoate on plants and animals, there is surprisingly little research on the effects of benzoate
69 and salicylate on the host microbiomes. In one study, aspirin inhibits the growth of
70 *Helicobacter pylori* and enhances the pathogen's sensitivity to antibiotics (23).

71 In *E. coli*, aromatic permeant acids such as salicylate and benzoate induce a large
72 number of low-level multidrug efflux systems, governed by the Mar operon (*marRAB*) as
73 well as additional unidentified mechanisms (24). Benzoate and salicylate upregulate
74 numerous genes of commensals and pathogens (25–28) including *acrAB*, *tolC*, and transport

bioRxiv preprint doi: https://doi.org/10.1101/063271; this version posted October 22, 2016. The copyright holder for this preprint (which was not certified by peer review) is the author/funder. All rights reserved. No reuse allowed without permission.

75 complexes that expel drugs across both the cytoplasmic and outer membrane. Mar-family
76 systems are widespread in bacterial genomes (29). Thus, in natural environments, aromatic
77 acids may serve bacteria as early warning signals for the presence of antibiotic-producing
78 competitors.

79 Mar-family regulons commonly involve extensive upregulation of many genes by a
80 small number of regulators. The *E. coli* regulator MarR represses expression of *marRAB*;
81 repression is relieved when MarR binds salicylate (30) or one of several less potent inducers
82 such as benzoate or 2,4-dinitrophenol. The upregulated MarA is an AraC-type global
83 regulator that differentially regulates approximately 60 genes (27, 31). Another AraC-type
84 regulator, Rob, activates *marRAB* (26, 32). MarA downregulates the acid-inducible Gad acid
85 fitness island (33). Gad includes glutamate decarboxylase (*gadA*) for extreme-acid survival
86 (32–34), as well as periplasmic chaperones *hdeA* and *hdeB* (35), and MDR loci *mdtE*, *mdtF*
87 (36). Besides Mar, short-term benzoate exposure up-regulates biofilm-associated genes
88 (*ymgABC*, *yhcN*), the fimbrial phase-variation regulator (*fimB*), and the cadmium stress
89 protein *yodA* (37).

90 Thus, aromatic acid-inducible drug resistance incurs high energy costs associated
91 with expression of so many genes, as well as the energy consumption by efflux pumps (38).
92 Given the high energy cost, bacteria face a tradeoff between inducible drug resistance and the
93 toxicity of the drugs (39). One would expect a high selective pressure for regulator alleles
94 that shift expression based on environmental factors. In fact, plate-based selection screens
95 using *lac* fusions readily pick up mutations in *marR* and in MarR-regulated genes (8).
96 Selective growth under antibiotic pressure leads to upregulation of *marRAB* (40).

bioRxiv preprint doi: https://doi.org/10.1101/063271; this version posted October 22, 2016. The copyright holder for this preprint (which was not certified by peer review) is the author/funder. All rights reserved. No reuse allowed without permission.

97 A powerful tool for dissecting long-term response to environmental stresses is
98 experimental evolution (41, 42). Experimental evolution procedures with *E. coli* have
99 included the adaptation to high temperatures (43), freeze-thaw cycles (44), high ethanol
100 concentrations (45), and acid (46–48). We developed a microplate dilution cycle in order to
101 generate evolving populations buffered at low pH (49). An advantage of our microplate
102 dilution cycle is that we propagate a number of populations directly in the microplate,
103 eliminating the intermediate stage of culture in flasks or tubes.
104 For the present study, we conducted experimental evolution of *E. coli* K-12 W3110 in
105 microplate well populations containing media buffered at pH 6.5 and supplemented with
106 increasing concentrations of benzoate (from 5 mM initially to 20 mM at 2,000 generations).
107 We sequenced genomes of selected isolates, then identified genetic variants using the *breseq*
108 pipeline (48–50). The *breseq* pipeline assembles a reference-based alignment to predict
109 mutations compared to a previously sequenced genome (NCBI GenBank accession number
110 NC_007779.1, *E. coli* K-12 W3110). Newer versions of *breseq* now predict structural
111 variations including large deletions, mobile element insertions, and gene duplications—all of
112 which account for much of the genetic diversity in evolved clones (50–53).
113 Our analysis unexpectedly shows that genetic adaptation to benzoate is associated
114 with loss or down-regulation of benzoate- and salicylate-inducible genes, including those that
115 encode multidrug resistance systems. The results have implications for evolution of the gut
116 microbiome during aspirin therapy. More broadly, our results suggest a way to amplify the
117 fitness costs of antibiotic resistance and possibly reverse antibiotic resistance in a
118 microbiome (54).
119

bioRxiv preprint doi: https://doi.org/10.1101/063271; this version posted October 22, 2016. The copyright holder for this preprint (which was not certified by peer review) is the author/funder. All rights reserved. No reuse allowed without permission.

120 MATERIALS AND METHODS

121 **Bacterial strains and media.** *Escherichia coli* K-12 W3110 (55) was the ancestral strain
122 of all benzoate-adapted populations. Additional strains derived from *E. coli* K-12 W3110
123 were isolated during the course of the evolution experiment (**Table 1**). Alleles with *kanR*
124 insertions were obtained from the Keio Collection (56) distributed by the Coli Genetic Stock
125 Center (CGSC). A *marR*::*kanR* strain was provided by Frederick R. Blattner, University of
126 Wisconsin-Madison.

127 Bacteria were cultured in LBK (10 g/L tryptone, 5 g/L yeast extract, 7.45 g/L KCl)
128 (57). Culture media were buffered with either 100mM piperazine-N,N'-bis(ethanesulfonic
129 acid) (PIPES; pKa= 6.8), 100 mM, 2-(N-morpholino)ethanesulfonic acid (MES; pKa= 5.96),
130 100 mM 3-morpholinopropane-1-sulfonic acid (MOPS; pKa= 7.20), 100 mM
131 homopiperazine-N,N'-bis-2-(ethanesulfonic acid) (HOMOPIPES; pKa = 4.55, 8.12), or 150
132 mM N-Tris(hydroxymethyl)methyl-3-aminopropanesulfonic acid (TAPS; pKa= 8.4). The
133 pH of the medium was adjusted as necessary with either 5 M HCl or 5 M KOH. Potassium
134 benzoate (referred to as benzoate), sodium salicylate (salicylate), potassium acetate,
135 potassium sorbate, chloramphenicol, or tetracycline was added before filter sterilization for
136 LBK media requiring various concentrations of acids or antibiotics. Temperature of
137 incubation was 37°C unless noted otherwise.

138 **Experimental Evolution.** Experimental evolution was conducted according to the
139 procedure of our low-pH laboratory evolution experiment (49) with modifications. Briefly,
140 24 cultures derived from the same ancestral strain (W3110, freezer stock D13) were cultured
141 continuously in increasing concentrations of benzoate for 2,000 generations (**Figure S1**). An
142 overnight culture of ancestral *Escherichia coli* K-12 W3110 was diluted 1:100 in LBK, pH

bioRxiv preprint doi: https://doi.org/10.1101/063271; this version posted October 22, 2016. The copyright holder for this preprint (which was not certified by peer review) is the author/funder. All rights reserved. No reuse allowed without permission.

143 6.5 100 mM PIPES, 5 mM potassium benzoate. Growth was recorded over 22 h in a
144 SpectraMax Plus384 MicroPlate reader (Molecular Devices). Every 15 minutes, the
145 microplate was shaken for 3 seconds and the OD_{450} of each culture was recorded. The
146 cultures were re-diluted 1:100 into fresh benzoate growth medium at the end of the daily
147 cycle. 100 µl glycerol (50% glycerol, 100 mM MES pH 6.5) was added to each well, after
148 which the microplate was frozen at -80°F (49). The number of generations of the exposed
149 cells was calculated based on the 1:100 daily dilution, resulting in a 100-fold daily growth to
150 achieve approximately 6.6 generations of binary fission (58). In the course of the 22-hour
151 cycle, all bacterial populations attained stationary phase densities. Plating representative
152 cultures showed that during the dilution cycle cell numbers increased from approximately
153 5×10^6 cells per ml to 5×10^8 cells per ml.
154 Over the course of the experiment, the benzoate concentration was increased in steps
155 when all populations of the plate had attained approximately100-fold stationary growth over
156 multiple dilution cycles (see **Figure S1**). After 60 generations, the benzoate was increased to
157 6 mM; 10 mM after 90 generations; 12 mM after 540 generations; 15 mM after 1,020
158 generations; 18 mM after 1,210 generations; 20 mM after 1,580 generations, to the
159 conclusion of the experiment with a cumulative 3,000 generations of growth. If the strains
160 had to be restarted from a frozen microplate, the frozen cultures were thawed and diluted
161 1:50 into fresh potassium benzoate growth media.
162 After 2,000 generations, microplates were taken from the freezer and samples from
163 specific wells were spread on LBK agar plates. Selected clones from each chosen well were
164 streaked three times and stored as freezer stocks. Clones were cultured in media at pH 6.5,
165 with 5 mM benzoate; all clones showed increased growth compared to ancestral strain

bioRxiv preprint doi: https://doi.org/10.1101/063271; this version posted October 22, 2016. The copyright holder for this preprint (which was not certified by peer review) is the author/funder. All rights reserved. No reuse allowed without permission.

166 W3110 (data not shown). For genome sequencing, eight clones were chosen in pairs from
167 each of four populations (clones A5-1, A5-2, C3-1, C3-2, E1-1, E1-2, G5-1, G5-2). A total
168 number of 24 clones (one from each population) were tested for sensitivity to
169 chloramphenicol (8 µg/ml) in 5 mM benzoate medium, pH 7.0. From these, eight additional
170 chloramphenicol-sensitive clones were selected for genomes sequencing (A1-1, A3-1, B1-1,
171 C1-1, D5-1, G3-1, H1-1, H3-1). All sixteen strains are identified in **Table 1**; and their
172 genomic mutations (compared to ancestral strain W3110) are presented in **Table S1**.
173 Mutations in six selected strains are presented in **Table 2**. These strains are color-coded
174 throughout our figures.

175 **Growth assays.** Growth curves were measured in the microplate reader at 37°C for
176 22 hours under various conditions of organic acids, pH values, and antibiotics. Strains were
177 cultured overnight in LBK pH 5.5 buffered with 100 mM MES; LBK pH 6.5 buffered with
178 100 mM PIPES; LBK pH 7.0 buffered with 100 mM MOPS; or LBK pH 8.5 buffered with
179 150 mM TAPS. Supplements included benzoate, salicylate, acetate, or sorbate, as stated in
180 figures. Overnight cultures were diluted 1:100 (1:200 for the antibiotic growth assays) into
181 the exposure media which included LBK pH 6.5 buffered with 100 mM PIPES; LBK pH 4.8,
182 100 mM HOMOPIPES; LBK pH 7.0, 100 mM MOPS; LBK pH 9.0, 150 mM TAPS; or LBK
183 pH 7.0, 100 mM MOPS. Every 15 minutes, the plate was shaken for 3 seconds and an
184 OD_{600} measurement was recorded. The growth rate k of each culture was calculated over the
185 period of 1-3 h, approximately the log phase of growth (34). The cell density E of each
186 culture was measured at 16 h unless stated otherwise.

187 **Genomic DNA extraction and sequencing.** Genomic DNA from benzoate-
188 evolved clones and from the ancestral wild type strain W3110 (freezer stock D13) was

bioRxiv preprint doi: https://doi.org/10.1101/063271; this version posted October 22, 2016. The copyright holder for this preprint (which was not certified by peer review) is the author/funder. All rights reserved. No reuse allowed without permission.

189 extracted using the DNeasy DNA extraction kit (Qiagen) and the MasterPure Complete DNA
190 and RNA Purification Kit (Epicentre). The DNA purity was confirmed by measuring the
191 260nm/280nm and 260nm/230nm absorbance ratios using a NanoDrop 2000
192 spectrophotometer (Thermo Fisher Scientific) and the concentration of the DNA was
193 measured using both the NanoDrop 2000 spectrophotometer (Thermo Fisher Scientific) and a
194 Qubit 3.0 Fluorometer (Thermo Fisher Scientific), according to manufacturer instructions.
195 The genomic DNA was sequenced by Michigan State University Research
196 Technology Support Facility Genomics Core. For Illumina MiSeq sequencing, libraries were
197 prepared using the Illumina TruSeq Nano DNA Library Preparation Kit. After library
198 validation and quantitation, they were pooled and loaded on an Illumina MiSeq flow cell.
199 Sequencing was done in a 2x250 bp paired-end format using an Illumina 500 cycle V2
200 reagent cartridge. Base calling was performed by Illumina Real Time Analysis (RTA)
201 v1.18.54 and output of RTA was demultiplexed and converted to FastQ format with Illumina
202 Bcl2fastq v1.8.4.
203 **Nucleotide sequence accession number.** Sequence data have been deposited in the
204 NCBI Sequence Read Archive (SRA) under accession number SRP074501.
205 **Sequence assembly and analysis using *breseq* computational pipeline.** The
206 computational pipeline *breseq* version 0.27.1 was used to assemble and annotate the resulting
207 reads of the evolved strains (50–52). The current *breseq* version detects IS element
208 insertions and IS-mediated deletions, as well as SNPs and other mutations (53). The reads
209 were mapped to the *E. coli* K-12 W3110 reference sequence (NCBI GenBank accession
210 number NC_007779.1) (59). Mutations were predicted by *breseq* by comparing the
211 sequences of the evolved isolates to that of the ancestral strain W3110, lab stock D13 (52).

bioRxiv preprint doi: https://doi.org/10.1101/063271; this version posted October 22, 2016. The copyright holder for this preprint (which was not certified by peer review) is the author/funder. All rights reserved. No reuse allowed without permission.

212 In order to visualize the assembly and annotations of our evolved isolate sequences mapped
213 to the reference *E. coli* K-12 W3110 genome, we used Integrative Genomics Viewer (IGV)
214 from the Broad Institute at MIT (60). Sequence identity of clones was confirmed by PCR
215 amplification of selected mutations.

216 **P1 phage transduction and strain construction.** P1 phage transduction was
217 conducted by standard procedures to replace a linked mutation with the ancestral non-
218 mutated allele, as well to construct knockout strains (49). Strains with *kanR* insertions (56)
219 were introduced into the evolved strain of choice or the ancestral strain W3110. Constructs
220 were confirmed by PCR amplification and Sanger sequencing of key alleles of donor and
221 recipient.

222 **MIC assays.** For assays of minimum inhibitory concentration (MIC) of antibiotics
223 (chloramphenicol or tetracycline) the strains were cultured in a microplate for 22 h in LBK
224 100 mM MOPS pH 7.0, 2 mM salicylate. The medium contained a range of antibiotic
225 concentration (μg/ml): 0, 1, 2, 4, 6, 8, 12, 16, 24. A positive result for growth was defined as
226 measurement of $OD_{600} \geq 0.05$. Each MIC was reported as the median value of 8 replicates.
227 For each antibiotic, three sets of 8 replicates were performed; that is, a total of 24 replicates
228 per strain.

229 **GABA assays.** The procedure for measuring GABA production via glutamate
230 decarboxylase was modified from that of Ref. (61). Strains were cultured overnight in LB
231 medium (10 g/L tryptone, 5 g/L yeast extract, 100 mM NaCl) buffered with 100 mM MES
232 pH 5.5. 10 mM glutamine was included, which the bacteria convert to glutamate, the
233 substrate of glutamate decarboxylase (62). For anaerobic culture, closed 9-ml screwcap tubes
234 nearly full of medium were incubated for 18 hours at 37°C. The pH of each sample was

bioRxiv preprint doi: https://doi.org/10.1101/063271; this version posted October 22, 2016. The copyright holder for this preprint (which was not certified by peer review) is the author/funder. All rights reserved. No reuse allowed without permission.

235 lowered with HCl to pH 2.0 for extreme-acid stress (63) and incubated 2 h with rotation. Cell
236 density (OD_{600}) was measured in microplate wells, in a SpectraMax plate reader. 1 ml of
237 each culture was pelleted in a microfuge. The supernatant was filtered and prepared for GC-
238 MS by EZ:faast amino acid derivatization (64). GABA concentration was calculated using a
239 standard solution prepared at a concentration of 200 nm/ml. GABA and other compounds
240 from the culture fluid were identified using NIST library analysis. GABA concentrations
241 were normalized to OD_{600} values of the overnight cultures before assay.
242

bioRxiv preprint doi: https://doi.org/10.1101/063271; this version posted October 22, 2016. The copyright holder for this preprint (which was not certified by peer review) is the author/funder. All rights reserved. No reuse allowed without permission.

243 RESULTS

244 **Experimental evolution of benzoate-tolerant strains.** We conducted experimental
245 evolution of *Escherichia coli* K-12 W3110 exposed to increasing concentrations of benzoic
246 acid, as described under Methods (**Figure S1**). Over the course of the experiment, bacteria
247 showed progressive increase of tolerance to benzoate tolerance, as measured by endpoint
248 culture density. Clones were sampled from microplate populations frozen at intervals over
249 the course of zero to 2,900 generations (**Fig. 1**). The clones were cultured in microplate wells
250 in media containing 20 mM benzoate at pH 6.5, and the cell density was measured at 16 h.
251 Over 1,400-2,900 generations the growth endpoints of evolved clones increased significantly
252 compared to that of the ancestor (**Fig. 1A**). A similar increase was observed for cell density
253 during growth with 10 mM salicylate (**Fig. 1B**). Thus overall, tolerance to benzoate and
254 salicylate increased over generations of exposure.

255 Since benzoate and salicylate induce multidrug resistance via the Mar regulon (24), it
256 was of interest to test drug resistance of the evolved clones. We measured growth in
257 chloramphenicol, an antibiotic that is effluxed by the MarA-dependent pump AcrA-AcrB-
258 TolC (27), which confers low-level resistance. For our experiment, the same set of clones
259 observed for growth in benzoate and salicylate were cultured in media containing 8 μg/μl
260 chloramphenicol (**Fig. 1C, 1D**). The media were adjusted to pH 7.0 for maximal growth and
261 contained a low concentration of benzoate or salicylate for induction of Mar regulon. Later
262 generations (1,900-2,900 gen) reached significantly lower cell density compared to that of
263 the ancestor W3110.

264 Our results suggest that populations evolving with benzoate experienced a tradeoff
265 between benzoate-salicylate tolerance and inducible chloramphenicol resistance. This

bioRxiv preprint doi: https://doi.org/10.1101/063271; this version posted October 22, 2016. The copyright holder for this preprint (which was not certified by peer review) is the author/funder. All rights reserved. No reuse allowed without permission.

266 tradeoff is confirmed by the plot of benzoate tolerance versus growth in chloramphenicol
267 (**Fig. 1E**). Clones from the ancestral strain W3110 (red circles) and early generations
268 (orange, generation 173; yellow, generation 399) showed little growth in 20 mM benzoate,
269 but most grew in 8 μg/ml chloramphenicol (reached OD_{600} values of at least 0.05). Middle-
270 generation clones (light green 897, dark green 1402) grew in benzoate to higher OD_{600} and
271 showed variable growth in chloramphenicol. By 2,900 generations (purple), all clones
272 reached OD_{600} values of at least 0.2 in 20 mM benzoate, but the clones barely grew at all in
273 chloramphenicol. Growth of evolved clones in salicylate, versus growth in salicylate and
274 chloramphenicol, showed a similar reciprocal relationship (**Fig. 1F**). Outliers appeared under
275 all conditions, as expected under selection pressure (65).

276 **Genome resequencing showed numerous SNPs, deletions, and IS5 insertion**
277 **mutations.** After 2,000 generations, 8 clones showing benzoate tolerance were chosen for
278 genome sequencing (described under Methods). An additional 24 clones (one from each
279 evolved population) were tested for chloramphenicol resistance; all were benzoate-tolerant
280 compared to strain W3110. Of these 24 clones, 8 were chosen for decreased resistance to
281 chloramphenicol. Both sets of 8 clones (16 in all) were streaked for isolation and established
282 as strains (**Table 1**). We used the *breseq* (version 0.27.1) computational pipeline to analyze
283 the mutation predictions of our resequenced genomes compared to the ancestral *E. coli*
284 W3110 (lab stock D13), assembled on the W3110 reference genome (59). More than 100
285 mutations were detected across the sixteen sequenced genomes (**Table S1**). Mutations found
286 in our resequenced lab stock D13 compared to the reference W3110 (**Table S2**) were filtered
287 from the results. The types of mutations that accumulated across the sixteen strains included
288 SNPs, small indels, insertion sequences (IS), and large IS-mediated deletions. Both coding

bioRxiv preprint doi: https://doi.org/10.1101/063271; this version posted October 22, 2016. The copyright holder for this preprint (which was not certified by peer review) is the author/funder. All rights reserved. No reuse allowed without permission.

289 changes and intergenic mutations were frequent. A large number of insertion knockouts were
290 mediated by mobile insertion sequence elements such as IS5 (66). An example, *gadX*::IS5
291 found in clone A5-1, is shown in **Fig. 2**. The inserted sequence, including *insH* plus IS5
292 flanking regions, was identical to those of 11 known IS5 inserts in the standard W3110
293 sequence; there was also a 4-bp duplication of the target site. Insertion sequence mobility is a
294 major source of evolutionary change in *E. coli* (67).

295 The 2,000-generation benzoate-adapted strains were grouped in six clades based on
296 shared mutations (**Table S1**); a representative member of each clade is shown in **Table 2**.
297 Most of the shared mutations originated within a population, as in the case of the two strains
298 taken from each of the A5, E1, and C3 populations; and from inadvertent cross-transfer
299 between microplate wells. For example, one population (G5) included a strain G5-2 that
300 shares mutations with the strains from the H1, H3 and G3 populations while sharing no
301 mutations with strain G5-1, from the G5 population. Note also that isolated shared mutations
302 can originate from the shared founder culture, or arise as independent genetic adaptations to a
303 common stress condition (65).

304 **Mutations appeared in Mar and other multidrug efflux systems.** Five of the six
305 clades showed mutations affecting the Mar regulon, as well as other MDR genes (**Table 2**).
306 Strain A5-1 had a 6,115-bp deletion including *marRAB* (*ydeA*, *marRAB*, *eamA*, *ydeEH*).
307 Regulators of Mar showed point mutations in strain G5-2 (*mar* paralog *rob*, Ref. (26)) and in
308 strain A1-1 (two-component activator *cpxA*, Ref. (68)). Additional mutations appeared in
309 other multidrug efflux systems: *emrA*, *emrY* (32, 69), *mdtA*, deletions covering *mdtEF* (69),
310 and *yeaS* (*leuE*) leucine export (70).

bioRxiv preprint doi: https://doi.org/10.1101/063271; this version posted October 22, 2016. The copyright holder for this preprint (which was not certified by peer review) is the author/funder. All rights reserved. No reuse allowed without permission.

311 The benzoate-evolved strains were tested by MIC assay for sensitivity to the
312 antibiotics chloramphenicol and tetracycline, whose resistance is inducible by benzoate
313 derivatives (**Table 3**). Sensitivity was assayed in the presence or absence of a Mar inducer, 2
314 mM salicylate. Salicylate increased the MIC for our ancestral strain W3110, for both
315 chloramphenicol and tetracycline. The W3110 *marA*::*kanR* construct showed less increase in
316 MIC for chloramphenicol. For tetracycline, our *marA* knockout strain showed no loss of
317 resistance; this may be due to induction of non-Mar salicylate-dependent resistance (24).
318 In the presence of salicylate, our evolved strains A1-1, A5-1, C3-1, and G5-2 showed
319 MIC levels half that of ancestor W3110. These lowered MIC levels were comparable to that
320 of a *marA* mutant, and only E1-1 showed chloramphenicol resistance equivalent to that of
321 W3110. In the absence of salicylate, the ancestral and evolved strains all showed lower MIC
322 values due to lack of inducer. The strain G5-2 showed slightly lower MIC than that of
323 W3110 (4 μg/m versus 6 μg/ml, respectively). Thus it is possible that G5-2 has lost an
324 additional component of chloramphenicol resistance that does not require salicylate
325 induction.
326 For tetracycline, salicylate-inducible resistance was less than that of W3110 for all of
327 our benzoate-evolved strains with the exception of strain E1-1. The tetracycline MIC values
328 however showed some variability; for all strains, uninducible MIC levels varied among trials
329 from 1-3 μg/ml. For further analysis, we focused on chloramphenicol.
330 **Mutations appeared in Gad acid resistance, RNAP, and fimbriae.** The Gad acid
331 resistance genes are induced during cytoplasmic acidification (37) and show regulation
332 intertwined with that of MDR systems (35). Strikingly, five of the six clades of our 16
333 sequenced strains showed a mutation in the Gad regulon (**Table 2**; **Table S1**). Strain E1-1

bioRxiv preprint doi: https://doi.org/10.1101/063271; this version posted October 22, 2016. The copyright holder for this preprint (which was not certified by peer review) is the author/funder. All rights reserved. No reuse allowed without permission.

334 had a 14,000-bp deletion mediated by the insertion sequence *insH* flanking the *gad* acid
335 fitness island (*gadXW*, *mdtFE*, *gadE*, *hdeDAB*, *yhiDF*, *slp*, *insH, yhiS*). Similarly, strain A1-1
336 showed a 10,738-bp deletion covering most of the *gad* region. A1-1 also had an insertion in
337 the *ariR* (*ymgB*) biofilm-dependent activator of Gad (37, 71). The *mdtFE* genes encode
338 components of the efflux pump MdtF-MdeE-TolC, which confers resistance to
339 chloramphenicol, as well as fluoroquinolones and other drugs (72). Thus, *gad* deletion might
340 explain chloramphenicol sensitivity of strain A1-1; but not E1-1, which was chloramphenicol
341 resistant despite the deletion. Other strains showed mutations in the *gadX* activator: A5-1
342 (IS5 insertion), G5-1 (missense L199F), and G5-2 (78-bp deletion). G5-2 also showed an *hfq*
343 point substitution, at a position known to affect function of RpoS (73), which activates Gad
344 (2).

345 The *gad* mutants showed different levels of GABA production by glutamate
346 decarboxylase (GadA) during extreme-acid exposure (incubation at pH 2) (**Fig. 3**). The two
347 strains with full Gad deletions (A1-1 and E1-1) produced no GABA, whereas strains with
348 *gadX* mutations (A5-1, G5-1, and G5-2) produced significantly less GABA than did the
349 ancestor W3110 (Friedman/Conover test). Only one representative strain, C3-1, showed no
350 Gad-related mutation; the nearest mutation was an IS5 insertion adjacent to *slp*. This strain
351 C3-1 produced GABA in amounts comparable to those of W3110.

352 Each benzoate-adapted strain also showed a mutation in an RNAP subunit (*rpoB,*
353 *rpoA*), a sigma factor (*rpoD, rpoS*) or an RNAP-associated helicase (*hepA*). These mutations
354 in the transcription apparatus are comparable to those we find under low-pH evolution (49).
355 Four of the six clades had mutations in fimbria subunit *fimA* or in regulators *fimB*, *fimE.*
356 Thus, benzoate exposure could select for loss of fimbriae synthesis. Other interesting

bioRxiv preprint doi: https://doi.org/10.1101/063271; this version posted October 22, 2016. The copyright holder for this preprint (which was not certified by peer review) is the author/funder. All rights reserved. No reuse allowed without permission.

357 mutations affected cell division (*ftsZ*), cell wall biosynthesis (*mrdA*), and envelope functions
358 (*ecpD, lptD*, *ybbP, yejM*, *yfhM*, *yqiGH*, and *rfaY*). The envelope mutations suggest responses
359 to benzoate effects on the outer membrane and periplasm.

360 **Benzoate-evolved strains showed increased growth rate and stationary phase cell**
361 **density.** In our evolution experiment, the microplate growth cycle (49) involves initially
362 oxygenated cultures, which become semianaerobic and ultimately enter stationary phase for
363 several hours. Thus, selection pressure occurs under changing conditions of oxygenation and
364 cell density. Dynamic conditions are relevant to host environments such as the intestinal
365 epithelium (74) and arterial plaque biofilms (75).

366 We observed the phases of growth for each benzoate-evolved strain, in order to
367 characterize the focus of selection pressure with respect to early growth rate, stationary-phase
368 cell density, and death phase. Observing the entire growth curve provides more information
369 than an endpoint MIC. Growth curves were conducted in microplate wells for each of the six
370 representative 2,000-generation benzoate-adapted strains. For each strain, eight replicate
371 wells of the microplate were inoculated alongside eight replicate wells of strain W3110, as
372 shown for strain G5-2 (**Fig. 4A**).

373 In the example shown, strain G5-2 maintained log-phase growth for approximately
374 four hours in the presence of 20 mM benzoate (0.42±0.5 gen/h, measured over times 1-3 h).
375 Strain G5-2 eventually reached a stationary-phase OD_{600} of approximately 1.0. By contrast,
376 ancestral strain W3110 grew more slowly (0.18±0.01 gen/h) and peaked at OD_{600}=0.5-0.7 by
377 about 8 h. After 8 h, W3110 entered a death phase as the cell density declined. The presence
378 of chloramphenicol, however, reversed the relative fitness of the two strains (**Fig. 4B**). The
379 benzoate-evolved strain barely grew, and 7 of 8 replicates entered death phase by 3-4 h. By

bioRxiv preprint doi: https://doi.org/10.1101/063271; this version posted October 22, 2016. The copyright holder for this preprint (which was not certified by peer review) is the author/funder. All rights reserved. No reuse allowed without permission.

380 contrast, the ancestor grew steadily to an OD_{600} of 0.5-0.6, a level that was sustained for
381 several hours.

382 At a lower concentration of chloramphenicol (4 μg/ml), the parental strain W3110
383 outgrew strain G5-2, even in the absence of benzoate inducer (**Fig. 4C**). This observation
384 confirms the MIC result (**Table 3**) that G5-2 shows loss of an unidentified means of
385 chloramphenicol resistance, independent of benzoate or salicylate. Other isolates showed
386 only loss of benzoate-inducible resistance (presented below).

387 The effect of various permeant acids was tested, in order to determine the specificity
388 of acid tolerance (**Fig. 5**). For all growth curves, statistical comparison was performed using
389 cell density values at 16 h. Each panel shows a curve with median cell density (at 16 h) for a
390 benzoate-evolved strain, as well as for strain W3110. Both benzoate and salicylate conditions
391 showed a marked fitness advantage for all six benzoate-evolved strains (**Fig. 5A, B**). Five of
392 the strains showed log-phase growth rates equivalent to each other, whereas G5-1 grew
393 significantly more slowly during log phase (Friedman, Conover tests; $p \leq 0.05$). All
394 benzoate-evolved strains grew faster than strain W3110. All six benzoate-evolved strains
395 reached equivalent plateau cell densities (OD_{600} values of approximately 1.0, with 20 mM
396 benzoate; 0.9, with 10 mM salicylate). By contrast, in 20 mM benzoate the strain W3110
397 entered death phase by 10 h. This observation strongly suggests that death rates contribute to
398 benzoate selection, besides the nominal 6.6 generations of growth per dilution cycle.

399 In the presence of aliphatic acids acetate or sorbate (**Fig. 5C, D**) no significant
400 difference was seen between growth of the ancestral strain W3110 and that of the benzoate-
401 evolved strains. Thus, the evolved fitness advantage is unlikely to result from cytoplasmic
402 pH depression but appears specific to the presence of aromatic acids benzoate or salicylate.

bioRxiv preprint doi: https://doi.org/10.1101/063271; this version posted October 22, 2016. The copyright holder for this preprint (which was not certified by peer review) is the author/funder. All rights reserved. No reuse allowed without permission.

403 Further testing with 40 μM carbonyl cyanide m-chlorophenyl hydrazone (the uncoupler
404 CCCP) showed no difference in growth rate or stationary-phase cell density among the
405 strains (data not shown). Thus, while decrease of proton motive force may be one factor it
406 cannot be the sole cause of the fitness advantage of our strains.

407 We also tested whether the benzoate-evolved strains showed any fitness advantage
408 with respect to pH stress. The strains were cultured in media buffered at pH7.0 (**Fig. 6A**) and
409 at pH 4.8 or pH 9.0 (**Fig. S2**). All of the benzoate-evolved strains grew similarly to the
410 ancestor at external pH values across the full range permitting growth. Thus, the fitness
411 advantage of the evolved strains was specific to the presence of benzoate or salicylate.

412 **Chloramphenicol inhibits growth of benzoate-evolved clones, despite benzoate**
413 **fitness advantage.** Since each of the six clades showed a mutation in an MDR gene or
414 regulator (discussed above), we characterized the growth profiles of all strains in the
415 presence of chloramphenicol (**Fig. 6B, C, D**). In the absence of benzoate or salicylate inducer
416 (**Fig. 6B**), all strains showed growth curves equivalent to that of W3110 or W3110
417 *marA*::*kanR* (which lacks the MarA activator of MDR efflux). Only the *marR*::*kanR* strains
418 (constitutive for activator *marA*) showed resistance. In the presence of benzoate (**Fig. 6C**) or
419 salicylate (**Fig. 6D**), the various benzoate-evolved strains reached different cell densities in
420 the presence of chloramphenicol. Panels presenting all 8 replicates of each strain are
421 presented in supplemental **Figures S3** and **S4**.

422 In the presence of chloramphenicol (with benzoate or salicylate) only strain E1-1
423 consistently grew at a rate comparable to W3110 (**Fig. 6C, D**). Strains A5-1 and G5-1 grew
424 to a lower density, comparable to that of the *marA*::*kanR* strain. Strains C3-1 and G5-2
425 showed hypersensitivity to chloramphenicol, with cell densities significantly below that of

bioRxiv preprint doi: https://doi.org/10.1101/063271; this version posted October 22, 2016. The copyright holder for this preprint (which was not certified by peer review) is the author/funder. All rights reserved. No reuse allowed without permission.

426 *marA*::*kanR*. The sensitivity of strain C3-1 is noteworthy given the absence of Mar or Gad
427 mutations. Another strain, G5-2, shows chloramphenicol sensitivity greater than the level that
428 would be predicted from loss of Rob activating MarA (25). Thus, the C3-1 and G5-2
429 genomes may reveal defects in other benzoate-inducible MDR genes, as yet unidentified.
430 **Mutations in *rob*, *gadX*, and *cpxA* do not affect chloramphenicol sensitivity or**
431 **benzoate tolerance.** Since five of the six benzoate-evolved strains showed defects affecting
432 Gad regulon, we tested the role of *gadX* in chloramphenicol resistance (**Fig. 7**). In the W3110
433 background, a *gadX*::*kanR* knockout (green) showed more sensitivity to chloramphenicol, as
434 did the construct W3110 *marA*::*kanR* (gray). Thus it is possible that GadX has some
435 uncharacterized role in chloramphenicol efflux, either via activation of the Mar regulon, or
436 else via activation of *mdtE*, *mdtF* in the Gad fitness island (36).
437 We also tested the role of *gadX* and *rob* in chloramphenicol sensitivity of the
438 benzoate-evolved strain G5-2. The G5-2 mutant alleles of Mar activator *rob* (S34P) and Gad
439 activator *gadX* (Δ78bp) were replaced by cotransduction. The ancestral alleles of *rob* and of
440 *gadX* were each moved into G5-2 by cotransduction with linked markers *yjjX790*::*kanR* and
441 *treF774*::*kanR* respectively. Constructs of G5-2 with allele replacements $gadX^+$ and rob^+
442 $gadX^+$ were cultured with chloramphenicol in the presence of 5 mM benzoate (**Fig. 7**). Both
443 constructs were as sensitive to chloramphenicol as the parental G5-2 strain. Furthermore,
444 strain G5-2 constructs with either rob^+, $gadX^+$, or rob^+ $gadX^+$ showed no significant loss of
445 benzoate tolerance compared to the parental strain G5-2 (data not shown). Thus, both the
446 benzoate fitness advantage and the chloramphenicol sensitivity of G5-2 must involve other
447 unidentified mutations in addition to *rob* or *gadX*.

bioRxiv preprint doi: https://doi.org/10.1101/063271; this version posted October 22, 2016. The copyright holder for this preprint (which was not certified by peer review) is the author/funder. All rights reserved. No reuse allowed without permission.

448 We also tested the effect of *cpxA*$^+$ on the benzoate fitness and chloramphenicol
449 sensitivity of strain A1-1. The parental allele of MDR regulator *cpxA* was moved from
450 W3110 into A1-1, replacing *cpxA*(N107S) with a marker *fdhD*::*kanR* linked to *cpxA*$^+$ (**Fig.**
451 **S5**). Growth curves were conducted as for **Figures 5 and 6**, tested under the conditions of 20
452 mM benzoate pH 6.5; benzoate with chloramphenicol; and salicylate with chloramphenicol.
453 Under all conditions, the cell density of strain W3110 *cpxA*::*kanR* (orange) showed no
454 difference from that of W3110; and strain JLS1607 (A1-1 *fdhD75*8::*kanR cpxA*+) (brown)
455 showed no difference from JLSK0001 (A1-1) (blue). Thus, strain A1-1 must also contain
456 benzoate-selected mutations in other unknown MDR genes.
457

bioRxiv preprint doi: https://doi.org/10.1101/063271; this version posted October 22, 2016. The copyright holder for this preprint (which was not certified by peer review) is the author/funder. All rights reserved. No reuse allowed without permission.

458 # DISCUSSION

459 In order to identify candidate genes for benzoate stress response, we sequenced the
460 genomes of experimentally evolved strains (41, 42, 46, 49, 76). We observed over 100
461 distinct mutations in the sequenced isolates after 2,000 generations, including a surprising
462 number of knockout alleles due to mobile elements (66, 67) in particular IS5 insertions and
463 IS5-mediated deletions (52). The *E. coli* K-12 W3110 genome contains many IS-elements,
464 including eight copies of IS1, five copies of IS2, and copies of other less well-studied IS
465 types where the most prevalent are IS1 and IS5 (59, 77, 78). Transposition of IS5 may be
466 induced by environmental factors such as motility conditions, which induce IS5 insertion
467 upstream of motility regulator *flhD* (79). Nonetheless, finding an additional 25 insertion
468 sequences under benzoate selection is remarkable. Our detection of such IS inserts was
469 enabled by use of the updated *breseq* pipeline (53).

470 Benzoate exposure decreases the cell's PMF while simultaneously upregulating
471 several regulons, including many involved in drug resistance. Our data suggests that benzoate
472 exposure selects for genetic changes in *E. coli* that result in, over time, the loss of
473 energetically costly systems such as Mar and other MDR regulons, as well as Gad acid-
474 inducible extreme-acid regulon. MarA is a potent transcriptional factor in *E. coli*,
475 upregulating numerous efflux pumps and virulence factors (8, 25, 27). The transcription and
476 translation of so many gene products would result in a considerable energy strain on the
477 individual cell.

478 Many MDR complexes are efflux pumps that spend PMF, which is diminished by
479 partial uncouplers such as benzoate or salicylate. The decreased energy expense could
480 explain the benzoate fitness advantage of strains that have broad-spectrum downregulation of

bioRxiv preprint doi: https://doi.org/10.1101/063271; this version posted October 22, 2016. The copyright holder for this preprint (which was not certified by peer review) is the author/funder. All rights reserved. No reuse allowed without permission.

481 Mar gene products, such as those we see in A5-1 and G5-2. At least one strain (G5-2) shows
482 detectable loss of chloramphenicol resistance in the absence of Mar inducer, suggesting loss
483 of constitutive MDR as well as the inducible system. Thus it might be possible for benzoate
484 and salicylate to select against a broad spectrum of drug resistance systems.

485 A similar energy load may occur under benzoate-depressed cytoplasmic pH, where
486 the Gad regulon is induced. Gad includes expression of numerous gene products such as
487 glutamate decarboxylase, whose activity enhances fitness only in extreme acid (pH 2) (35)
488 and which breaks down valuable amino acids. Thus the deletion of the *gad* region (seen in
489 strains A1-1 and E1-1) could eliminate a fruitless energy drain. For comparison, we find
490 similar Gad deletions in our pH 4.6 evolution experiment (He et al. manuscript in
491 preparation) but not in our evolution experiment conducted at pH 9.2 (unpublished). This
492 implies that both pH 4.6 and benzoate/pH 6.5 induce Gad under conditions where glutamate
493 decarboxylase fails to help the cell, and thus the energy-expensive Gad expression is selected
494 against.

495 The Gad region also includes genes encoding an MDR complex (*mdtEF*) (36); and a
496 *gadX* knockout showed some loss of chloramphenicol resistance (**Fig. 7**). Note however that
497 our E1-1 strain retains chloramphenicol resistance despite Gad deletion, whereas strain C3-1
498 (chloramphenicol sensitive) possesses the entire Gad region except for a possible defect in
499 *slp*, encoding an acid-resistance outer membrane protein. Thus, Gad mutations alone cannot
500 explain the chloramphenicol sensitivities of our strains.

501 Another possible consequence of energy stress is the loss of fimbriae synthesis
502 (strains A5-1, C3-1, E1-1, G5-1). Avoiding fimbriae production could save energy for
503 benzoate-stressed cells. Fim genes also show deletion under evolution at pH 9.2 (Issam

bioRxiv preprint doi: https://doi.org/10.1101/063271; this version posted October 22, 2016. The copyright holder for this preprint (which was not certified by peer review) is the author/funder. All rights reserved. No reuse allowed without permission.

504 Hamdallah, unpublished), but not at pH 4.6. This suggests a hypothesis that fimbriae
505 biosynthesis is dependent less on pH than on the protonmotive force (PMF), which is
506 depleted both by benzoate and at high external pH, a condition that decreases PMF (5).
507 The progressive loss of antibiotic resistance is a remarkable consequence of benzoate
508 selection, evident as early as 1,500 generations (**Fig. 1**). Several observations point to the
509 existence of inducible MDR systems yet to be discovered. Strains C3-1 and G5-2 show
510 hypersensitivity to chloramphenicol, beyond the level of sensitivity seen in a *marA* knockout
511 (**Fig. 6C, D; Fig. S3**). Furthermore, the reversion of mutant alleles of *rob*, *gadX*, and *cpxA* do
512 not diminish the phenotypes of the 2,000-generation strains. It is likely that these alleles
513 conferred a fitness advantage early on in our evolution experiment (65) but have since been
514 superseded by further mutations in as yet unidentified players in drug resistance.
515 The fitness tradeoff between drug resistance and benzoate/salicylate exposure has
516 implications for the human microbiome. Mar and homologs such as Mex are reported in
517 numerous bacteria, including proteobacteria and *Bacteroides fragilis* (80, 81). Salicylate is a
518 plant defense molecule commonly obtained via human diets rich in fruits and vegetables (82,
519 83). Aspirin is deacetylated in the liver and stomach, forming salicylic acid, the primary
520 therapeutic agent (84). As a membrane-permeant acid, salicylic acid permeates human tissues
521 nonspecifically. Both food-related and aspirin-derived salicylates come in contact with
522 enteric gut bacteria, where they would be expected to activate Mar-like antibiotic resistance
523 systems. Commonly prescribed for cardiac health, aspirin releases salicylate at plasma levels
524 of approximately 0.2 mM (16, 19, 20, 22).
525 Intestinal salicylate levels are poorly understood, but even lower concentrations of
526 this antimicrobial agent could have fitness effects. For comparison, small concentrations of

bioRxiv preprint doi: https://doi.org/10.1101/063271; this version posted October 22, 2016. The copyright holder for this preprint (which was not certified by peer review) is the author/funder. All rights reserved. No reuse allowed without permission.

527 antibiotics, well below the MIC, can select for resistance (85, 86). Similarly, it may be that
528 small concentrations of a resistance-reversing agent such as salicylate have a significant
529 fitness cost for MDR bacteria. Furthermore, the effective concentration of permeant acids
530 such as salicylate is amplified exponentially by the pH difference across the bacterial plasma
531 membrane. Even mild acidity in the intestinal lumen (pH 6-6.5) could amplify the bacterial
532 cytoplasmic concentration of a permeant acid by 10- to 30-fold.

533 Aspirin therapy is known to prevent clotting by inactivation of human
534 cyclooxygenase, leading to suppression of prostaglandins. There is little attention, however,
535 to the possible effects of aspirin on human-associated bacteria. Gram-negative pathogens
536 such as *Pseudomonas* are found in arterial plaques and associated with heart attacks (75).
537 Aspirin-derived salicylate in plasma might provide a fitness cost for such bacteria. Aspirin
538 also prevents colon cancer, by some unknown mechanism (16, 20). Colon cancer depends on
539 colonic bacteria and the formation of biofilms (87, 88).

540 Long-term salicylate exposure via aspirin therapy may select a microbiome that is
541 salicylate-tolerant but drug-sensitive. A salicylate-adapted microbiome may confer the
542 benefit of excluding drug-resistant pathogens that lack salicylate tolerance. In blood plasma,
543 salicylate levels might help exclude bacteria from arterial plaques. An adverse consideration,
544 however, is that the salicylate-adapted microbiome of the colon may be more vulnerable to
545 high dose antibiotic therapy. For the future, we are testing these speculative possibilities in
546 host microbial models.

547

bioRxiv preprint doi: https://doi.org/10.1101/063271; this version posted October 22, 2016. The copyright holder for this preprint (which was not certified by peer review) is the author/funder. All rights reserved. No reuse allowed without permission.

548 **Acknowledgements**

549 We thank Zachary Blount, Jeff Barrick, Michael Harden, Rohan Maddamsetti, Peter Lund,

550 and Bradley Hartlaub for valuable discussions. We thank Anna Tancredi for testing the *gadX*

551 mutant. This work was funded by grant MCB-1329815 from the National Science

552 Foundation, and by the Kenyon College Summer Science Scholars.

553

bioRxiv preprint doi: https://doi.org/10.1101/063271; this version posted October 22, 2016. The copyright holder for this preprint (which was not certified by peer review) is the author/funder. All rights reserved. No reuse allowed without permission.

REFERENCES

1. **Kanjee U**, **Houry WA**. 2013. Mechanisms of acid resistance in *Escherichia coli*. Annu Rev Microbiol **67**:65–81.

2. **Foster JW**. 2004. *Escherichia coli* acid resistance: Tales of an amateur acidophile. Nat Rev Microbiol **2**:898–907.

3. **Audia JP**, **Webb CC**, **Foster JW**. 2001. Breaking through the acid barrier: An orchestrated response to proton stress by enteric bacteria. Int J Med Microbiol **291**:97–106.

4. **Krulwich TA**, **Sachs G**, **Padan E**. 2011. Molecular aspects of bacterial pH sensing and homeostasis. Nat Rev Microbiol **9**:330–43.

5. **Slonczewski JL**, **Fujisawa M**, **Dopson M**, **Krulwich TA**. 2009. Cytoplasmic pH measurement and homeostasis in bacteria and archaea.Adv Microb Physiol.

6. **Qin J**, **Li R**, **et al.** 2010. A human gut microbial gene catalogue established by metagenomic sequencing. Nature **464**:59–67.

7. **Slonczewski JL**, **Macnab RM**, **Alger JR**, **Castle AM**. 1982. Effects of pH and repellent tactic stimuli on protein methylation levels in *Escherichia coli*. J Bacteriol **152**:384–399.

8. **Rosner JL**, **Slonczewski JL**. 1994. Dual regulation of inaA by the multiple antibiotic resistance (Mar) and superoxide (SoxRS) stress response systems of *Escherichia coli*. J Bacteriol **176**:6262–6269.

9. **Lee CH**, **Oon JSH**, **Lee KC**, **Ling MHT**. 2012. *Escherichia coli* ATCC 8739 adapts to the presence of sodium chloride, monosodium glutamate, and benzoic acid after extended culture. ISRN Microbiol **2012**.

10. **Beales N**. 2004. Adaptation of microorganisms to cold temperatures, weak acid preservatives, low pH, and osmotic stress: A review. Compr Rev Food Sci Food Saf **3**:1–20.

bioRxiv preprint doi: https://doi.org/10.1101/063271; this version posted October 22, 2016. The copyright holder for this preprint (which was not certified by peer review) is the author/funder. All rights reserved. No reuse allowed without permission.

11. **Wilks JC**, **Slonczewski JL**. 2007. pH of the cytoplasm and periplasm of *Escherichia coli*: Rapid measurement by green fluorescent protein fluorimetry. J Bacteriol **189**:5601–5607.

12. **Lennerz B**, **Vafai SB**, **Delaney NF**, **Clish CB**, **Deik AA**, **Pierce KA**, **Ludwig D s.**, **Mootha VK**. 2015. Effects of sodium benzoate, a widely used food preservative, on glucose homeostatsis and metabolic profiles in humans. Mol Genet Metab **114**:73–79.

13. **An C**, **Mou Z**. 2011. Salicylic acid and its function in plant immunity. J Integr Plant Biol **53**:412–428.

14. **Du L**, **Ali GS**, **Simons KA**, **Hou J**, **Yang T**, **Reddy ASN**, **Poovaiah BW**. 2009. Ca2+/calmodulin regulates salicylic-acid-mediated plant immunity. Nature **457**:1154–1158.

15. **Hawley S a**, **Fullerton MD**, **Ross F a**, **Schertzer JD**, **Chevtzoff C**, **Walker KJ**, **Peggie MW**, **Zibrova D**, **Green K a**, **Mustard KJ**, **Kemp BE**, **Sakamoto K**, **Steinberg GR**, **Hardie DG**. 2012. The ancient drug salicylate directly activates AMP-activated protein kinase. Science (80-) **336**:918–922.

16. **Paterson JR**, **Lawrence JR**. 2001. Salicylic acid: a link between aspirin, diet and the prevention of colorectal cancer. QJM **94**:445–448.

17. **Paterson JR**, **Baxter G**, **Dreyer JS**, **Halket JM**, **Flynn R**, **Lawrence JR**. 2008. Salicylic acid sans aspirin in animals and man : Persistence in fasting and biosynthesis from benzoic acid. J Agric Food Chem **56**:11648–11652.

18. **Spadafranca a**, **Bertoli S**, **Fiorillo G**, **Testolin G**, **Battezzati A**. 2007. Circulating salicylic acid is related to fruit and vegetable consumption in healthy subjects. Br J Nutr **98**:802–806.

19. **Patrono C**, **García Rodríguez LA**, **Landolfi R**, **Baigent C**. 2005. Low-dose aspirin for the prevention of atherothrombosis. N Engl J Med **353**:2373–2383.

20. **Patrono C**. 2013. Low-dose aspirin in primary prevention: cardioprotection, chemoprevention, both, or neither? Eur Hear J **34**:3403–3411.

21. **Hundal RS**, **Petersen KF**, **Mayerson AB**, **Randhawa PS**, **Inzucchi S**, **Shoelson SE**,

bioRxiv preprint doi: https://doi.org/10.1101/063271; this version posted October 22, 2016. The copyright holder for this preprint (which was not certified by peer review) is the author/funder. All rights reserved. No reuse allowed without permission.

Shulman GI. 2002. Mechanism by which high-dose aspirin improves glucose metabolism in type 2 diabetes. J Clin Invest **109**:1321–1326.

22. **Ahmed N**, **Meek J**, **Davies GJ**. 2010. Plasma salicylate level and aspirin resistance in survivors of myocardial infarction. J Thromb Thrombolysis **29**:416–420.

23. **Wang WH**, **Wong WM**, **Dailidiene D**, **Berg DE**, **Gu Q**, **Lai KC**, **Lam SK**, **Wong BCY**. 2003. Aspirin inhibits the growth of *Helicobacter pylori* and enhances its susceptibility of antimicrobial agents. Gut **52**:490–495.

24. **Cohen SP**, **Levy SB**, **Foulds J**, **Rosner JL**. 1993. Salicylate induction of antibiotic resistance in *Escherichia coli*: Activation of the *mar* operon and a *mar*-independent pathway. J Bacteriol **175**:7856–7862.

25. **Duval V**, **Lister IM**. 2014. MarA, SoxS and Rob of *Escherichia coli* – Global regulators of multidrug resistance, virulence and stress response. Int J Biotechnol Wellness Ind **2**:101–124.

26. **Chubiz LM**, **Rao C V.** 2010. Aromatic acid metabolites of *Escherichia coli* K-12 can induce the *marRAB* operon. J Bacteriol **192**:4786–4789.

27. **Ruiz C**, **Levy SB**. 2010. Many chromosomal genes modulate MarA-mediated multidrug resistance in *Escherichia coli*. Antimicrob Agents Chemother **54**:2125–2134.

28. **Critzner FJ**, **Dsouza DH**, **Golden DA**. 2008. Transcription analysis of *stx1*, *marA*, and *eaeA* genes in *Escherichia coli* O157:H7 treated with sodium benzoate. J Food Prot **71**:1469–74.

29. **Perera IC**, **Grove A**. 2010. Molecular mechanisms of ligand-mediated attenuation of DNA binding by MarR family transcriptional regulators. J Mol Cell Biol **2**:243–254.

30. **Alekshun MN**, **Levy SB**, **Mealy TR**, **Seaton BA**, **Head JF**. 2001. The crystal structure of MarR, a regulator of multiple antibiotic resistance, at 2.3 Å resolution. Nat Struct Mol Biol **8**:710–714.

31. **Barbosa TM, Levy SB**. 2000. Differential expression of over 60 chromosomal genes in *Escherichia coli* by constitutive expression of MarA. J Bacteriol **182**:3467–3474.

bioRxiv preprint doi: https://doi.org/10.1101/063271; this version posted October 22, 2016. The copyright holder for this preprint (which was not certified by peer review) is the author/funder. All rights reserved. No reuse allowed without permission.

32. **Grkovic S**, **Brown MH**, **Skurray RA**, **Repressor A**, **Subtilis B**. 2002. Regulation of bacterial drug export systems. Microbiolgy Mol Biol Rev **66**:671–701.

33. **Ruiz C**, **McMurry LM**, **Levy SB**. 2008. Role of the multidrug resistance regulator MarA in global regulation of the *hdeAB* acid resistance operon in *Escherichia coli*. J Bacteriol **190**:1290–1297.

34. **Deininger KNW**, **Horikawa A**, **Kitko RD**, **Tatsumi R**, **Rosner JL**, **Wachi M**, **Slonczewski JL**. 2011. A requirement of tolc and MDR efflux pumps for acid adaptation and GadAB induction in *Escherichia coli*. PLoS One **6**:1–7.

35. **Mates AK**, **Sayed AK**, **Foster JW**. 2007. Products of the *Escherichia coli* acid fitness island attenuate metabolite stress at extremely low pH and mediate a cell density-dependent acid resistance. J Bacteriol **189**:2759–2768.

36. **Nishino K**, **Senda Y**, **Yamaguchi A**. 2008. The AraC-family regulator GadX enhances multidrug resistance in *Escherichia coli* by activating expression of *mdtEF* multidrug efflux genes. J Infect Chemother **14**:23–29.

37. **Kannan G**, **Wilks JC**, **Fitzgerald DM**, **Jones BD**, **Bondurant SS**, **Slonczewski JL**. 2008. Rapid acid treatment of *Escherichia coli*: transcriptomic response and recovery. BMC Microbiol **8**.

38. **Anes J**, **McCusker MP**, **Fanning S**, **Martins M**. 2015. The ins and outs of RND efflux pumps in Escherichia coli. Front Microbiol **6**:1–14.

39. **Wood KB**, **Cluzel P**. 2012. Trade-offs between drug toxicity and benefit in the multi-antibiotic resistance system underlie optimal growth of *E. coli*. BMC Syst Biol **6**:48.

40. **Weiss SJ**, **Mansell TJ**, **Mortazavi P**, **Knight R**, **Gill RT**. 2016. Parallel mapping of antibiotic resistance alleles in *Escherichia coli*. PLoS One **11**:1–17.

41. **Blount ZD**, **Borland CZ**, **Lenski RE**. 2008. Historical contingency and the evolution of a key innovation in an experimental population of *Escherichia coli*. Proc Natl Acad Sci U S A **105**:7899–7906.

42. **Blount ZD**, **Barrick JE**, **Davidson CJ**, **Lenski RE**. 2012. Genomic analysis of a key innovation in an experimental *Escherichia coli* population. Nature **489**:513–518.

bioRxiv preprint doi: https://doi.org/10.1101/063271; this version posted October 22, 2016. The copyright holder for this preprint (which was not certified by peer review) is the author/funder. All rights reserved. No reuse allowed without permission.

43. **Riehle MM**, **Bennett AF**, **Lenski RE**, **Long AD**. 2003. Evolutionary changes in heat-inducible gene expression in lines of *Escherichia coli* adapted to high temperature. Physiol Genomics **14**:47–58.

44. **Sleight SC**, **Lenski RE**. 2007. Evolutionary adaptation to freeze-thaw-growth cycles in Escherichia coli. Physiol Biochem Zool **80**:370–385.

45. **Goodarzi H**, **Bennett BD**, **Amini S**, **Reaves ML**, **Hottes AK**, **Rabinowitz JD**, **Tavazoie S**. 2010. Regulatory and metabolic rewiring during laboratory evolution of ethanol tolerance in *E. coli*. Mol Syst Biol **6**:378.

46. **Dragosits M**, **Mattanovich D**. 2013. Adaptive laboratory evolution – principles and applications for biotechnology. Microb Cell Fact **12**.

47. **Hughes BS**, **Cullum AJ**, **Bennett AF**. 2007. Evolutionary adaptation to environmental pH in experimental lineages of *Escherichia coli*. Evolution (N Y) **61**:1725–1734.

48. **Johnson MD**, **Bell J**, **Clarke K**, **Chandler R**, **Pathak P**, **Xia Y**, **Marshall RL**, **Weinstock GM**, **Loman NJ**, **Winn PJ**, **Lund PA**. 2014. Characterization of mutations in the PAS domain of the EvgS sensor kinase selected by laboratory evolution for acid resistance in Escherichia coli. Mol Microbiol **93**:911–927.

49. **Harden MM**, **He A**, **Creamer K**, **Clark MW**, **Hamdallah I**, **Martinez KA**, **Kresslein RL**, **Bush SP**, **Slonczewski JL**. 2015. Acid-Adapted Strains of *Escherichia coli* K-12 Obtained by Experimental Evolution. Appl Environ Microbiol **81**:1932–1941.

50. **Barrick JE**, **Colburn G**, **Deatherage DE**, **Traverse CC**, **Strand MD**, **Borges JJ**, **Knoester DB**, **Reba A**, **Meyer AG**. 2014. Identifying structural variation in haploid microbial genomes from short-read resequencing data using *breseq*. BMC Genomics **15**:1039.

51. **Deatherage DE**, **Traverse CC**, **Wolf LN**, **Barrick JE**. 2015. Detecting rare structural variation in evolving microbial populations from new sequence junctions using *breseq*. Front Genet **5**:1–16.

52. **Deatherage DE**, **Barrick JE**. 2014. Identification of mutations in laboratory-evolved

bioRxiv preprint doi: https://doi.org/10.1101/063271; this version posted October 22, 2016. The copyright holder for this preprint (which was not certified by peer review) is the author/funder. All rights reserved. No reuse allowed without permission.

microbes from next-generation sequencing data using *breseq*. Methods Mol Biol **1151**:165–188.

53. **Tenaillon O**, **Barrick JE**, **Ribeck N**, **Deatherage DE**, **Blanchard JL**, **Dasgupta A**, **Wu GC**, **Schneider D**, **Lenski RE**. 2016. Tempo and mode of genome evolution in a 50,000 - generation experiment. bioRXiv Prepr http//dx.doi.org/101101/036806 **536**:1–21.

54. **Andersson DI**, **Hughes D**. 2010. Antibiotic resistance and its cost: is it possible to reverse resistance? Nat Rev Microbiol **8**:260–71.

55. **Smith MW**, **Neidhardt FC**. 1983. Proteins induced by aerobiosis in *Escherichia coli*. J Bacteriol **154**:344–350.

56. **Baba T**, **Ara T**, **Hasegawa M**, **Takai Y**, **Okumura Y**, **Baba M**, **Datsenko KA**, **Tomita M**, **Wanner BL**, **Mori H**. 2006. Construction of *Escherichia coli* K-12 in-frame, single-gene knockout mutants: the Keio collection. Mol Syst Biol **2**.

57. **Maurer LM**, **Yohannes E**, **Bondurant SS**, **Radmacher M**, **Slonczewski JL**. 2005. pH regulates genes for flagellar motility, catabolism, and oxidative stress in *Escherichia coli* K-12. J Bacteriol **187**:304–319.

58. **Lenski RE**, **Rose MR**, **Simpson SC**, **Tadler SC**. 1991. Long-term Experimental Evolution in *Escherichia coli* I. Adaptation and Divergence During 2,000 Generations. Am Nat **138**:1315–1341.

59. **Hayashi K**, **Morooka N**, **Yamamoto Y**, **Fujita K**, **Isono K**, **Choi S**, **Ohtsubo E**, **Baba T**, **Wanner BL**, **Mori H**, **Horiuchi T**. 2006. Highly accurate genome sequences of *Escherichia coli* K-12 strains MG1655 and W3110. Mol Syst Biol **2**:2006.0007.

60. **Thorvaldsdóttir H**, **Robinson JT**, **Mesirov JP**, **Thorvaldsdottir H**, **Robinson JT**, **Mesirov JP**. 2013. Integrative genomics viewer (IGV): High-performance genomics data visualization and exploration. Brief Bioinform **14**:178–192.

61. **Ma Z**, **Gong S**, **Richard H**, **Tucker DL**, **Conway T**, **Foster JW**. 2003. GadE (YhiE) activates glutamate decarboxylase-dependent acid resistance in *Escherichia coli* K-12. Mol Microbiol **49**:1309–1320.

bioRxiv preprint doi: https://doi.org/10.1101/063271; this version posted October 22, 2016. The copyright holder for this preprint (which was not certified by peer review) is the author/funder. All rights reserved. No reuse allowed without permission.

62. **Lu P**, **Ma D**, **Chen Y**, **Guo Y**, **Chen G-Q**, **Deng H**, **Shi Y**. 2013. L-glutamine provides acid resistance for *Escherichia coli* through enzymatic release of ammonia. Cell Res **23**:635–44.

63. **Lin J**, **Smith MP**, **Chapin KC**, **Baik HS**, **Bennett GN**, **Foster JW**. 1996. Mechanisms of acid resistance in enterohemorrhagic *Escherichia coli*. Appl Environ Microbiol **62**:3094–3100.

64. **Badawy AA-B**. 2012. The EZ:Faast family of amino acid analysis kits: application of the GC-FID kit for rapid determination of plasma tryptophan and other amino acids. Methods Mol Biol **828**:153–64.

65. **Maddamsetti R**, **Lenski RE**, **Barrick JE**. 2015. Adaptation, clonal interference, and frequency-dependent interactions in a long-term evolution experiment with *Escherichia coli*. Genetics **200**:619–631.

66. **Schnetz K**, **Rak B**. 1992. IS5: a mobile enhancer of transcription in *Escherichia coli*. Proc Natl Acad Sci U S A **89**:1244–1248.

67. **Schneider D**, **Lenski RE**. 2004. Dynamics of insertion sequence elements during experimental evolution of bacteria. Res Microbiol **155**:319–327.

68. **Weatherspoon-Griffin N**, **Yang D**, **Kong W**, **Hua Z**, **Shi Y**. 2014. The CpxR/CpxA two-component regulatory system up-regulates the multidrug resistance cascade to facilitate *Escherichia coli* resistance to a model antimicrobial peptide. J Biol Chem **289**:32571–32582.

69. **Li X-Z**, **Plésiat P**, **Nikaido H**. 2015. The challenge of efflux-mediated antibiotic resistance in gram-negative bacteria. Clin Microbiol Rev **28**:337–418.

70. **Kutukova EA**, **Livshits VA**, **Altman IP**, **Ptitsyn LR**, **Zyiatdinov MH**, **Tokmakova IL**, **Zakataeva NP**. 2005. The yeaS (leuE) gene of *Escherichia coli* encodes an exporter of leucine, and the Lrp protein regulates its expression. FEBS Lett **579**:4629–4634.

71. **Lee J**, **Page R**, **García-Contreras R**, **Palermino JM**, **Zhang XS**, **Doshi O**, **Wood TK**, **Peti W**. 2007. Structure and function of the *Escherichia coli* Protein YmgB: A protein critical for biofilm formation and acid-resistance. J Mol Biol **373**:11–26.

bioRxiv preprint doi: https://doi.org/10.1101/063271; this version posted October 22, 2016. The copyright holder for this preprint (which was not certified by peer review) is the author/funder. All rights reserved. No reuse allowed without permission.

72. **Trittler R**, **Kern W V**, **Bohnert A**, **Schuster S**, **Fa E**. 2007. Altered spectrum of multidrug resistance associated with a single point mutation in the *Escherichia coli* RND-type MDR efflux pump YhiV (MdtF). J Antimicrob Chemother **59**:1216–1222.

73. **Ziolkowska K**, **Derreumaux P**, **Folichon M**, **Pellegrini O**, **Boni I V**, **Hajnsdorf E**. 2006. Hfq variant with altered RNA binding functions. Nucleic Acids Res **34**:709–720.

74. **Zheng L**, **Kelly CJ**, **Colgan SP**. 2015. Physiologic hypoxia and oxygen homeostasis in the healthy intestine. A Review in the Theme: Cellular Responses to Hypoxia. Am J Physiol Cell Physiol **309**:C350-60.

75. **Lanter BB**, **Sauer K**, **Davies DG**. 2014. Bacteria present in carotid arterial plaques are found as biofilm deposits which may contribute to enhanced risk of plaque rupture. MBio **5**:1–8.

76. **Barrick JE**, **Lenski RE**. 2013. Genome dynamics during experimental evolution. Nat Rev Genet **14**:827–839.

77. **Herring CD**, **Raghunathan A**, **Honisch C**, **Patel T**, **Applebee MK**, **Joyce AR**, **Albert TJ**, **Blattner FR**, **van den Boom D**, **Cantor CR**, **Palsson BØ**. 2006. Comparative genome sequencing of *Escherichia coli* allows observation of bacterial evolution on a laboratory timescale. Nat Genet **38**:1406–1412.

78. **Blattner FR**, **Plunkett G**, **Bloch CA**, **Perna NT**, **Burland V**, **Riley M**, **Collado-Vides J**, **Glasner JD**, **Rode CK**, **Mayhew GF**, **Gregor J**, **Davis NW**, **Kirkpatrick HA**, **Goeden MA**, **Rose DJ**, **Mau B**, **Shao Y**. 1997. The complete genome sequence of *Escherichia coli* K-12. Science (80-) **277**:1453–1462.

79. **Wang X**, **Wood TK**. 2011. IS*5* inserts upstream of the master motility operon *flhDC* in a quasi-Lamarckian way. ISME J **5**:1517–1525.

80. **Pumbwe L**, **Skilbeck CA**, **Wexler HM**. 2007. Induction of multiple antibiotic resistance in *Bacteroides fragilis* by benzene and benzene-derived active compounds of commonly used analgesics, antiseptics and cleaning agents. J Antimicrob Chemother **60**:1288–1297.

81. **Ueda O**, **Wexler HM**, **Hirai K**, **Shibata Y**, **Yoshimura F**, **Fujimura S**. 2005.

bioRxiv preprint doi: https://doi.org/10.1101/063271; this version posted October 22, 2016. The copyright holder for this preprint (which was not certified by peer review) is the author/funder. All rights reserved. No reuse allowed without permission.

Sixteen homologs of the mex-type multidrug resistance efflux pump in *Bacteroides fragilis*. Antimicrob Agents Chemother **49**:2807–2815.

82. **Tomas-Barberan FA**, **Clifford MN**. 2000. Review Dietary hydroxybenzoic acid derivatives – nature , occurrence and dietary burden **1032**.

83. **Blacklock CJ**, **Lawrence JR**, **Wiles D**, **Malcolm EA**, **Gibson IH**, **Kelly CJ**, **Paterson JR**. 2001. Salicylic acid in the serum of subjects not taking aspirin. Comparison of salicylic acid concentrations in the serum of vegetarians, non-vegetarians, and patients taking low dose aspirin. J Clin Pathol **54**:553–555.

84. **Needs C**, **Brooks P**. 1985. Clinical pharmacokinetics of the salicylates. Clin Pharmacokinet **10**:164–177.

85. **Gullberg E**, **Cao S**, **Berg OG**, **Ilbäck C**, **Sandegren L**, **Hughes D**, **Andersson DI**. 2011. Selection of resistant bacteria at very low antibiotic concentrations. PLoS Pathog **7**:1–9.

86. **Andersson DI**, **Hughes D**. 2014. Microbiological effects of sublethal levels of antibiotics. Nat Rev Microbiol **12**:465–78.

87. **Sears CL**, **Garrett WS**. 2014. Microbes, microbiota, and colon cancer. Cell Host Microbe **15**:317–328.

88. **Johnson CH**, **Dejea CM**, **Sears CL**, **Johnson CH**, **Dejea CM**, **Edler D**, **Hoang LT**, **Santidrian AF**, **Felding BH**, **Casero RA**, **Pardoll DM**, **White JR**, **Patti GJ**, **Sears CL**, **Siuzdak G**. 2015. Metabolism links bacterial biofilms and colon carcinogenesis. Cell Metab **21**:891–897.

bioRxiv preprint doi: https://doi.org/10.1101/063271; this version posted October 22, 2016. The copyright holder for this preprint (which was not certified by peer review) is the author/funder. All rights reserved. No reuse allowed without permission.

TABLES

Table 1. Bacterial strains used in this study.

Strain	Population number or allele	Source
W3110	*Escherichia coli* K-12 stock #D13	Fred Neidhardt
JLSK0001	W3110 Benzoate-evolved **A1-1**	This study
JLSK0011	W3110 Benzoate-evolved **A3-1**	This study
JLSK0022	W3110 Benzoate-evolved **A5-1**	This study
JLSK0023	W3110 Benzoate-evolved **A5-2**	This study
JLSK0002	W3110 Benzoate-evolved **B1-1**	This study
JLSK0003	W3110 Benzoate-evolved **C1-1**	This study
JLSK0014	W3110 Benzoate-evolved **C3-1**	This study
JLSK0015	W3110 Benzoate-evolved **C3-2**	This study
JLSK0026	W3110 Benzoate-evolved **D5-1**	This study
JLSK0006	W3110 Benzoate-evolved **E1-1**	This study
JLSK0007	W3110 Benzoate-evolved **E1-2**	This study
JLSK0010	W3110 Benzoate-evolved **H1-1**	This study
JLSK0020	W3110 Benzoate-evolved **H3-1**	This study
JLSK0019	W3110 Benzoate-evolved **G3-1**	This study
JLSK0030	W3110 Benzoate-evolved **G5-1**	This study
JLSK0031	W3110 Benzoate-evolved **G5-2**	This study
JW5249-1	BW25113 *marA752*::*kanR*	(56)
JLS1506	W3110 *marA752*::*kanR*	This study
MG1655 *marR*::*kanR*	MG1655 *marR*::*kanR*	Fred Blattner

bioRxiv preprint doi: https://doi.org/10.1101/063271; this version posted October 22, 2016. The copyright holder for this preprint (which was not certified by peer review) is the author/funder. All rights reserved. No reuse allowed without permission.

JLS1610	W3110 *marR*::*kanR*	This study
JW3484-1	BW25113 *gadX771*::*kanR*	(56)
JLS1517	W3110 *gadX771*::*kanR*	This study
JW5801-1	BW25113 *yjjX790*::*kanR*	(56)
JLS1514	W3110 *yjjX790*::*kanR rob+*	This study
JW3487-1	BW25113 *treF774*::*kanR*	(56)
JLS1612	G5-2 *treF774*::*kanR* *gadX*$^+$	This study
JLS1613	G5-2 *yjjX790*::*frt* *rob*$^+$ *treF774*::kanR *gadX*$^+$	This study
JW3866-3	BW25113 *fdhD758*::*kanR*	(56)
JLS1607	A1-1 *fdhD758*::*kanR cpxA+*	This study

bioRxiv preprint doi: https://doi.org/10.1101/063271; this version posted October 22, 2016. The copyright holder for this preprint (which was not certified by peer review) is the author/funder. All rights reserved. No reuse allowed without permission.

Table 2. Mutations in representative benzoate-evolved genomes compared to the genome of *E. coli* W3110.

JLS	K0001	K0022	K0014	K0006	K0030	K0031			
Position	**A1-1**	**A5-1**	**C3-1**	**E1-1**	**G5-1**	**G5-2**	**Mutation**	**Annotation**	**Gene**
56,273	■						G→A	L279L (CTC→CTT)	imp (lptD) ←
62,682		■					+G	coding (583/2907 nt)	hepA ←
105,411				■			G→A	G36D (GGT→GAT)	ftsZ →
156,056					■		T→G	N49T (AAT→ACT)	ecpD ←
444,525				■			T→G	intergenic (+127/+1)	yajQ → / ← yajR
490,544		■					Δ6 bp	intergenic (+61/‑87)	ybaN → / → apt
490,998				■			Δ1 bp	coding (363/552 nt)	apt →
520,989				■			G→T	P450P (CCG→CCT)	ybbP →
556,778	■		■	■			A→C	F63V (TTC→GTC)	folD ←
573,671		■					T→A	intergenic (+109/+289)	ybcQ → / ← insH
666,783					■		A→T	D619E (GAT→GAA)	mrdA ←
683,143						92%	Δ5,116 bp	insH-3 IS5‑mediated	[hscC]–gltI
755,210					99%		IS5 +8bp	intergenic (+147/‑374)	gltA ← / sdhC →
909,411						■	G→A	P102P (CCC→CCT)	ltaE ←
991,031			■				IS5 (–) +4 bp	intergenic (‑253/‑10)	pncB ← / → pepN
1,213,665	■						(C)8→9	intergenic (‑85/+615)	elbA ← / ← ycgX
1,218,024	■						IS5 (+) +4 bp	coding (79‑82/267 nt)	ariR (ymgB) →
1,337,160						■	G→A	intergenic (+617/‑385)	cysB → / → acnA
1,349,606	98%						IS5 +5 bp	coding (1021/1935 nt)	rnb ←
1,372,264			■				A→G	E112G (GAG→GGG)	ycjM →
1,459,205					■		G→A	G354G (GGG→GGA)	paaE →
1,485,978						■	C→A	R383S (CGT→AGT)	hrpA →
1,549,542		■					IS5 (–) +4 bp	coding (428‑431/3048 nt)	fdnG →
1,553,926						■	T→C	intergenic (+221/+186)	fdnI → / ← yddM
1,565,001				■			A→G	intergenic (‑211/+47)	ddpX ← / ← dos
1,574,188						■	IS5 (+) +4 bp	coding (2726‑2729/2796 nt)	pqqL ←
1,592,479						■	C→A	intergenic (‑229/+89)	yneL ← / ← hipA
1,618,943		■					Δ6,115 bp	coding inclusive deletion	ydeA–marCRAB-ydeH
1,704,037						■	Δ1 bp	coding (91/1002 nt)	add →
1,772,079			98%				IS5 +4 bp	intergenic (+179/‑250)	ydiK → / ydiL →
1,822,769		99%					IS5 +4 bp	coding (160/1359 nt)	chbC ←
1,881,543						■	IS186/IS421 (+) +6 bp	coding (115‑120/360 nt)	yeaR ←
1,882,210				■			G→A	L88L (CTC→CTT)	yeaS ←
1,908,956			■				IS5 (–) +4 bp	coding (191‑194/210 nt)	cspC ←
1,909,258		■					IS1 (+) +9 bp	coding (40‑48/144 nt)	yobF ←
1,932,183				■			Δ1 bp	coding (279/291 nt)	yebG ←
2,093,073		■					G→A	E249K (GAA→AAA)	hisG →
2,156,723						■	C→A	L191M (CTG→ATG)	mdtA →
2,434,645				■			A→T	V347E (GTG→GAG)	purF ←
2,447,095						■	C→T	intergenic (‑44/‑115)	fabB ← / → trmC
2,487,190				■			IS5 (+) +4 bp	coding (430‑433/1539 nt)	emrY ←
2,646,569	■						C→A	E1459* (GAG→TAG)	yfhM ←
2,739,952					■		C→A	intergenic (‑146/‑64)	aroF ← / → yfiL
2,810,717					■		IS2 (–) +5 bp	coding (635‑639/1173 nt)	emrA →
2,865,825					■		A→T	I89N (ATC→AAC)	rpoS ←
2,931,775	■						C→A	P190P (CCG→CCT)	fucA ←
3,104,794						■	G→A	G142D (GGC→GAC)	nupG →
3,169,126					■		A→C	T215P (ACA→CCA)	qseB →
3,187,655			■				IS5 (–) +4 bp	coding (1600‑1603/2466 nt)	yqiG →
3,188,360					■		IS5 (–) +4 bp	coding (2305‑2308/2466 nt)	yqiG →
3,189,138					■		IS5 (+) +4 bp	coding (602‑605/750 nt)	yqiH →
3,212,340						■	A→C	D213A (GAC→GCC)	rpoD →
3,241,721		■					G→T	L84M (CTG→ATG)	uxaA ←
3,277,113		99%					INDEL +5 bp	coding (257/336 nt)	prlF →
3,277,128				■			(TTCAACA)2→3	coding (272/336 nt)	sohA →
3,454,320	■						C→T	G373S (GGC→AGC)	rpoB ←
3,532,025	■						A→G	N107S (AAC→AGC)	cpxA →

bioRxiv preprint doi: https://doi.org/10.1101/063271; this version posted October 22, 2016. The copyright holder for this preprint (which was not certified by peer review) is the author/funder. All rights reserved. No reuse allowed without permission.

3,840,032							IS5 (–) +4 bp	coding (583-586/699 nt)	rfaY →
3,909,304							IS5 (+) +4 bp	intergenic (-20/-343)	xylF ← / → xylA
3,948,766							G→A	R320H (CGT→CAT)	bcsB →
3,974,240							Δ14,146 bp	insH IS5-mediated	gadXW–mdtFE-hdeDAB-yhiS
3,974,646				Δ			Δ78 bp	coding (42-119/825 nt)	gadX →
3,975,201				Δ			G→T	L199F (TTG→TTT)	gadX →
3,975,230				Δ			IS5 (+) +4 bp	coding (626-629/825 nt)	gadX →
3,976,435				Δ			Δ10,738 bp	insH-mediated	gadW–slp
3,986,969	Δ			Δ			Δ204 bp	insH-mediated	slp ← / → insH
4,114,118							C→A	intergenic (-171/-149)	yrfF ← / → nudE
4,136,677							G→T	V191V (GTC→GTA)	frlD ←
4,200,197							A→C	K271Q (AAA→CAA)	rpoA →
4,218,986							IS5 (–) +4 bp :: Δ4	intergenic (+187/-79)	metA → / → aceB
4,221,755							G→A	A353T (GCA→ACA)	aceA →
4,297,865							+T	intergenic (+136/-206)	nrfG → / → gltP
4,397,133							C→T	intergenic (+18/-19)	glyV → / → glyX
4,397,136							A→G	intergenic (+21/-16)	glyV → / → glyX
4,405,094							G→A	V43M (GTG→ATG)	hfq →
4,485,284							IS5 (–) +4 bp	coding (875-878/1197 nt)	yjgN →
4,495,464							IS5 (+) +4 bp	coding (353-356/999 nt)	idnR ←
4,546,700							IS5 (–) +4 bp	intergenic (+461/-14)	fimB → / → fimE
4,546,841							IS5 (–) +4 bp	coding (125-128/597 nt)	fimE →
4,547,128							IS5 (–) +4 bp	coding (412-415/597 nt)	fimE →
4,547,650							Δ1 bp	intergenic (+337/-145)	fimE → / → fimA
4,547,860							(TCCCTCAGTTCTA CAGCGGCTCTG)1→2	coding (66/549 nt)	fimA →
4,626,165							C→G	C201W (TGC→TGG)	deoD →
4,639,891							A→G	S34P (TCC→CCC)	rob ←

[1] NCBI reference strain NCBI NC_007779.1. "Δ" indicates mutation site is absent within a larger deleted region. Percentage scores indicate *breseq* calls less than 100%. Background colors designate strains. Mutation annotations: Red = changed base pairs; green = synonymous mutation; blue = missense mutation; purple = IS-mediated deletion; and * = nonsense mutation. Mutations present in our laboratory stock strain W3110-D13 compared to the NCBI reference strain (**Table S2**) are omitted from Table 2.

bioRxiv preprint doi: https://doi.org/10.1101/063271; this version posted October 22, 2016. The copyright holder for this preprint (which was not certified by peer review) is the author/funder. All rights reserved. No reuse allowed without permission.

Table 3. MIC (minimum inhibitory concentration) of benzoate-evolved strains in the antibiotics chloramphenicol and tetracycline, with or without salicylate.*

	Chloramphenicol		Tetracycline	
	No inducer	2 mM salicylate	No inducer	2 mM salicylate
W3110	6	16	1	4
marA::kanR	6	8	1.5	4
A1-1	6	8	1.5	2
A5-1	6	8	2.5	1
C3-1	6	8	1	3
E1-1	6	16	1	4
G5-1	7	12	1	2
G5-2	4	8	1	2

*Cultured in LBK 100 mM MOPS pH 7.0, +/- 2 mM salicylate, for 22 h. Positive for growth was defined as cell density at 22 h ($OD_{600} \geq 0.05$). Concentration (µg/ml) represents median value of 8 replicates. The experiment shown represents one of three trials overall.

bioRxiv preprint doi: https://doi.org/10.1101/063271; this version posted October 22, 2016. The copyright holder for this preprint (which was not certified by peer review) is the author/funder. All rights reserved. No reuse allowed without permission.

FIGURES

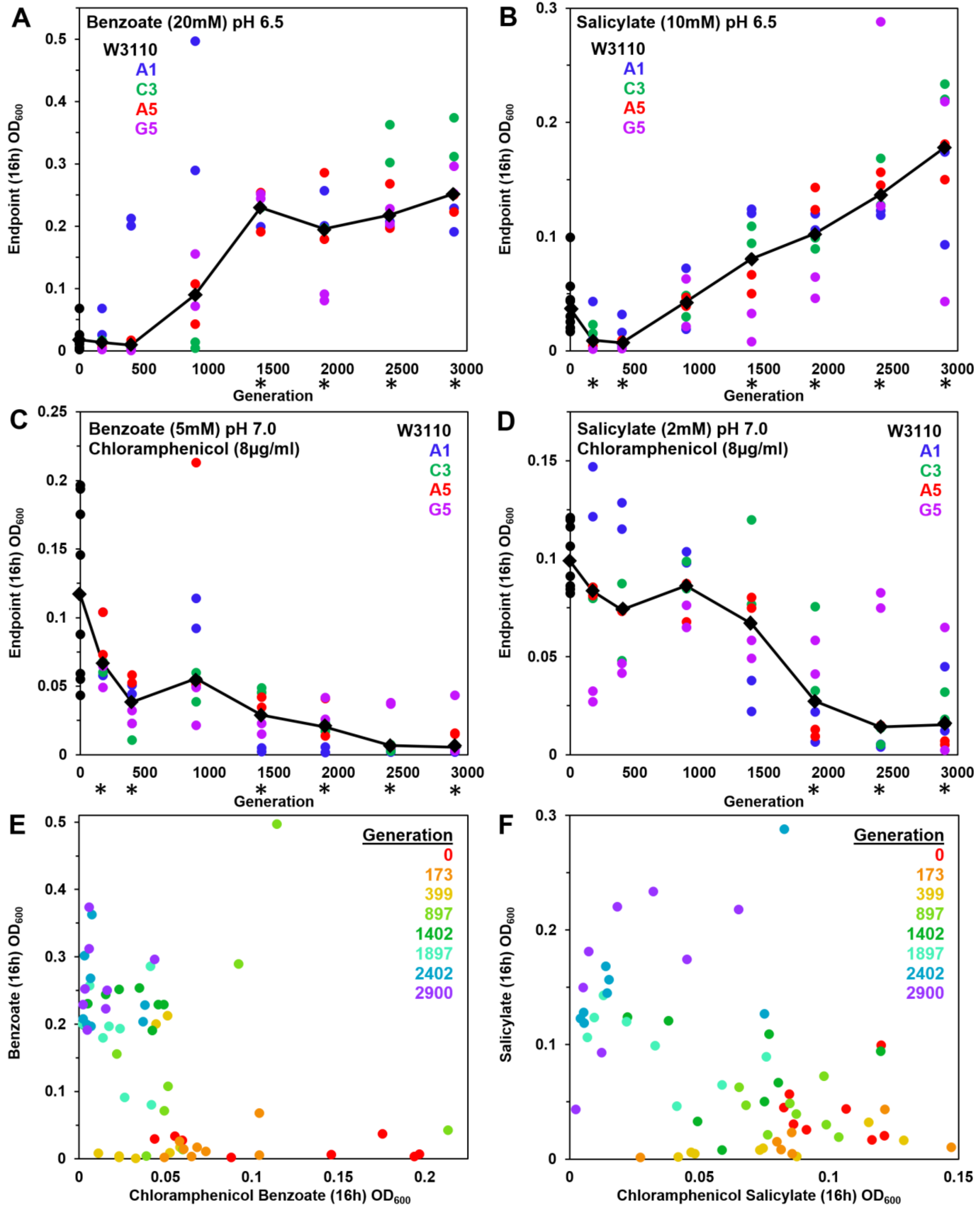

bioRxiv preprint doi: https://doi.org/10.1101/063271; this version posted October 22, 2016. The copyright holder for this preprint (which was not certified by peer review) is the author/funder. All rights reserved. No reuse allowed without permission.

FIG 1 Growth measured after generations of repeated dilution and culture in 5-20 mM benzoate. Benzoate-evolved strains were isolated from frozen microplates, selecting 2 different clones from each of 4 populations. Clones from each plate generation were cultured at 37ºC in a column of microplate wells; cell density "E" values (OD_{600}) were obtained at 16 h. For panels A-D, the colored dots represent lineages of evolved clones collected from distinct well populations (A1, C3, A5, G5) after different numbers of generations as indicated on the X axis. Diamonds indicate median cell density for each generation tested. Bracket indicates generations for which the 16-h cell density differed significantly from that of the ancestral strain W3110, in 2 out of 3 trials of the entire microplate experiment. For each microplate trial, the Friedman test was performed with post-hoc Conover pairwise comparisons and Holm-Bonferroni adjusted p-values. LBK media contained: **A.** 100 mM PIPES pH 6.5 with 20 mM benzoate (diluted 1:200 from overnight cultures with 5mM benzoate). **B.** 100 mM PIPES pH 6.5 with 10 mM salicylate (diluted 1:200 from overnight cultures in 2 mM salicylate). **C.** 100 mM MOPS pH 7.0 with 5 mM benzoate, 8 µg/ml chloramphenicol (diluted 1:200 from overnight cultures lacking chloramphenicol). **D.** 100 mM MOPS pH 7.0 with 2 mM salicylate, 8 µg/ml chloramphenicol (diluted 1:200 from overnight cultures lacking chloramphenicol). **E.** Plot with linear regression of 16-h cell-density values for 20 mM benzoate and for 5 mM benzoate, 8 µg/ml chloramphenicol exposures. **F.** Plot with linear regression of 16-h cell-density values for 10 mM salicylate and for 2 mM salicylate, 8 µg/ml chloramphenicol exposures.

bioRxiv preprint doi: https://doi.org/10.1101/063271; this version posted October 22, 2016. The copyright holder for this preprint (which was not certified by peer review) is the author/funder. All rights reserved. No reuse allowed without permission.

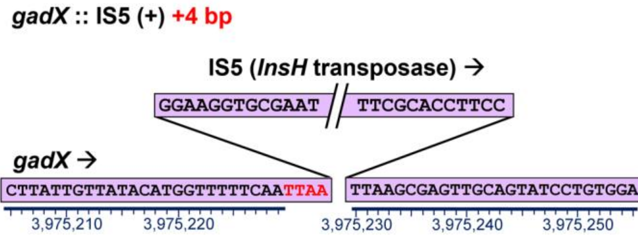

FIG 2 New insertion of IS5 within *gadX* including a 4-bp duplication of the target site, in the A5-1 genome at position 3,975,230.

bioRxiv preprint doi: https://doi.org/10.1101/063271; this version posted October 22, 2016. The copyright holder for this preprint (which was not certified by peer review) is the author/funder. All rights reserved. No reuse allowed without permission.

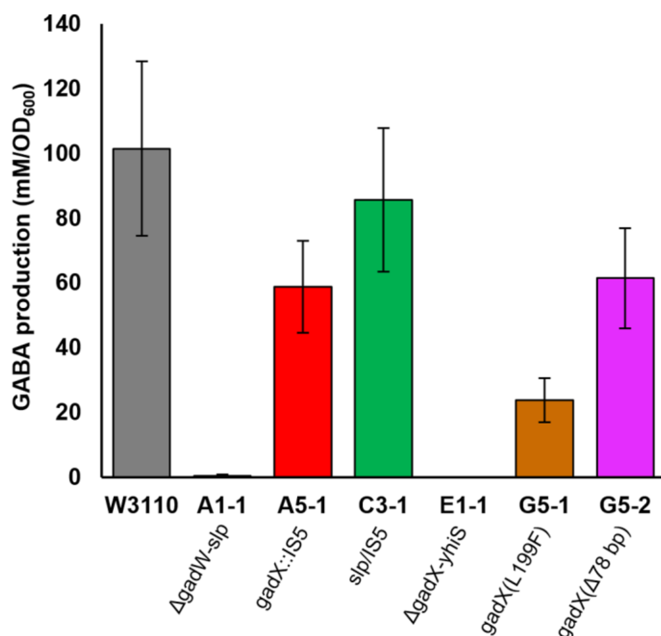

FIG 3 GABA produced by benzoate-evolved strains compared to W3110. Anaerobic overnight cultures in LB 10 mM glutamine, 100 mM MES pH 5.5 were adjusted with HCl to pH 2. After 2 h incubation, bacteria were pelleted and supernatant culture fluid was derivatized using EZ:faast (see Methods). GABA was quantified via GC/MS, and values were normalized to the cell density of the overnight culture. Error bars represent SEM (n=7 or 8). Genetic annotations are from Table 1.

bioRxiv preprint doi: https://doi.org/10.1101/063271; this version posted October 22, 2016. The copyright holder for this preprint (which was not certified by peer review) is the author/funder. All rights reserved. No reuse allowed without permission.

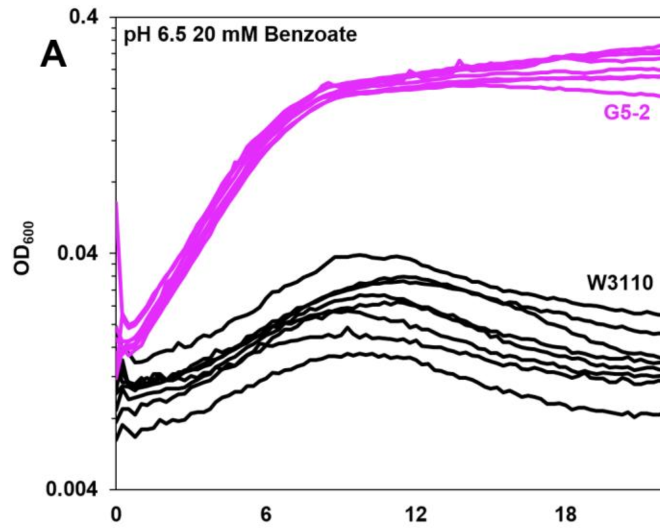

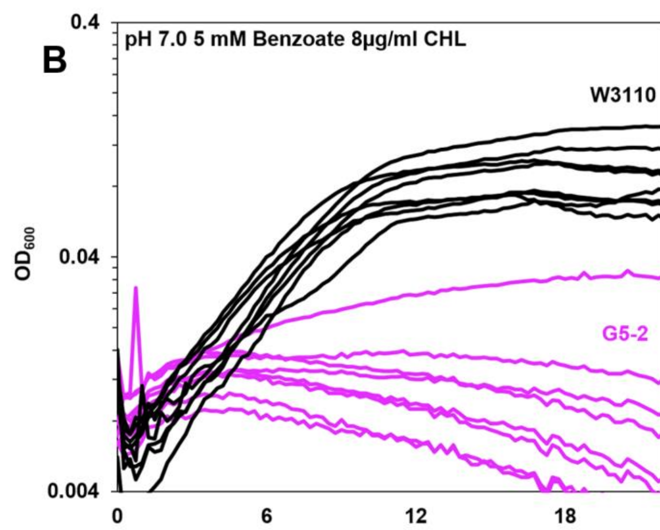

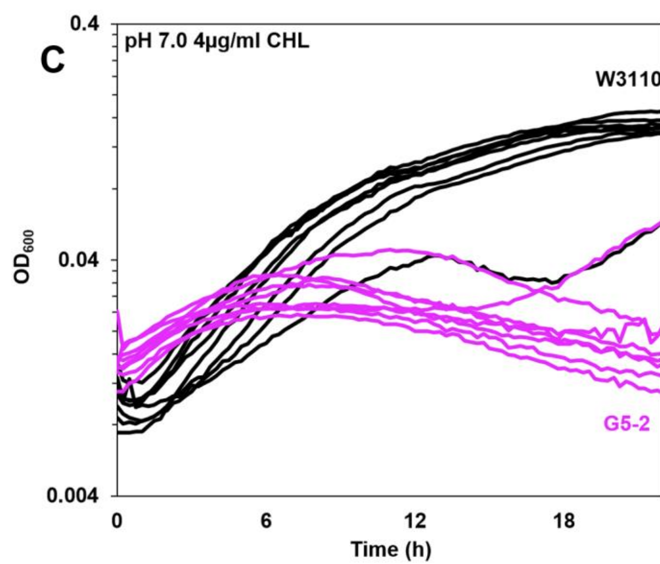

bioRxiv preprint doi: https://doi.org/10.1101/063271; this version posted October 22, 2016. The copyright holder for this preprint (which was not certified by peer review) is the author/funder. All rights reserved. No reuse allowed without permission.

FIG 4 Benzoate-evolved strain G5-2 outgrows ancestor W3110 in presence of benzoate, but grows poorly in benzoate with chloramphenicol. Growth medium was LBK with (**A**) 100 mM PIPES, 20 mM benzoate pH 6.5, (**B**) 100 mM MOPS, 5 mM benzoate pH 7.0, 8 μg/ml chloramphenicol (CHL). (**C**) 100 mM MOPS, pH 7.0, 4 μg/ml CHL. For each strain, 8 replicate curves from microplate wells are shown. For strains G5-2 and W3110 in each panel, cell density values post log-phase (OD_{600} at 16 h) were ranked and compared by Friedman test; post-hoc Conover pairwise comparisons were conducted with Holm-Bonferroni adjusted p-values.

bioRxiv preprint doi: https://doi.org/10.1101/063271; this version posted October 22, 2016. The copyright holder for this preprint (which was not certified by peer review) is the author/funder. All rights reserved. No reuse allowed without permission.

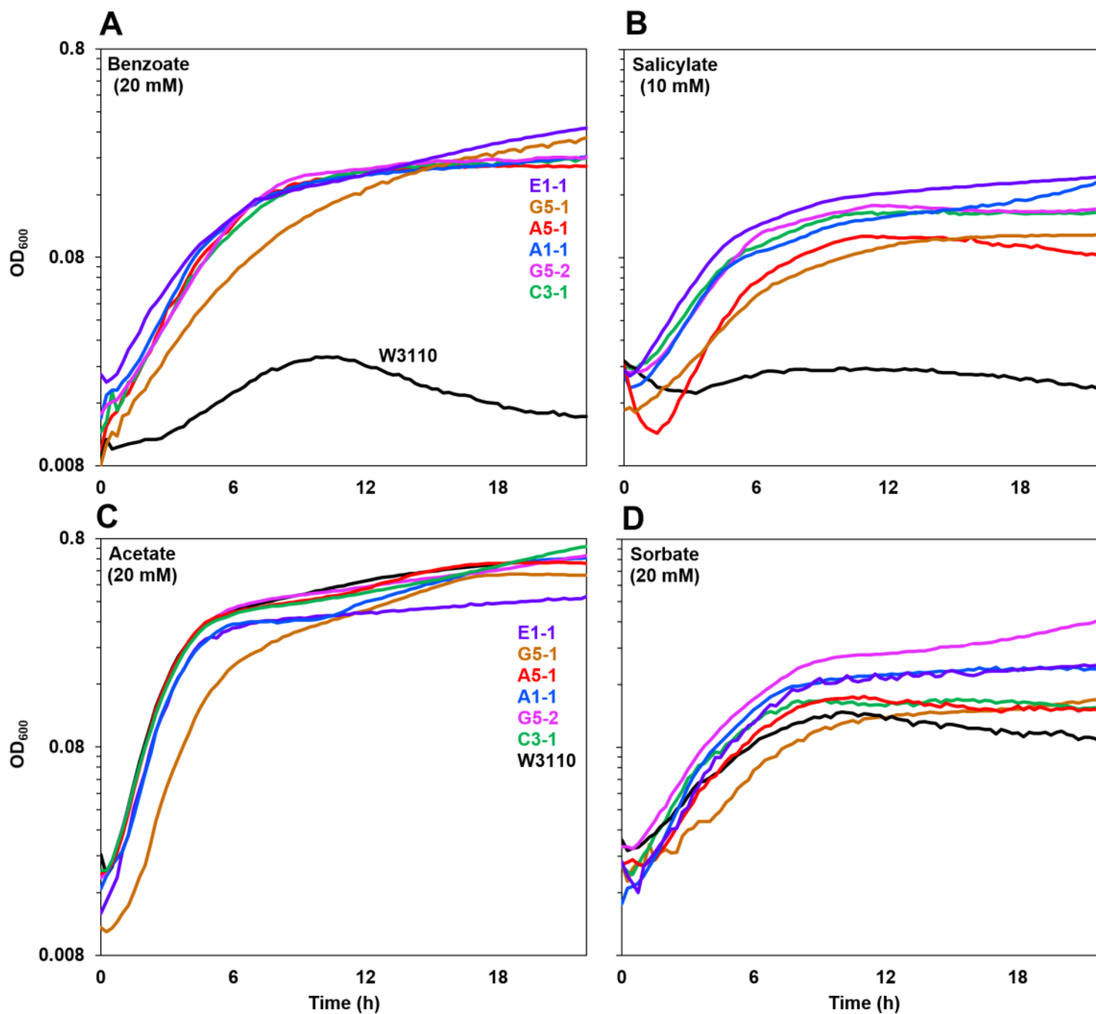

FIG 5 Benzoate-evolved strains all outgrow ancestor in benzoate or salicylate but not in acetate or sorbate. Growth curves of benzoate-evolved strains (colored curves) and ancestor (black curve) in LBK 100 mM PIPES pH 6.5 with (A) 20mM benzoate, (B) 10 mM salicylate, (C) 20mM acetate, or (D) 20 mM sorbate. For each strain, a curve with median cell density at 16 h is shown. Panels A and B (but not C and D) showed significantly lower 16-h cell density for the ancestral W3110 strain than for benzoate-evolved strains (Friedman test; post-hoc Conover pairwise comparisons with Holm-Bonferroni adjusted p-values).

bioRxiv preprint doi: https://doi.org/10.1101/063271; this version posted October 22, 2016. The copyright holder for this preprint (which was not certified by peer review) is the author/funder. All rights reserved. No reuse allowed without permission.

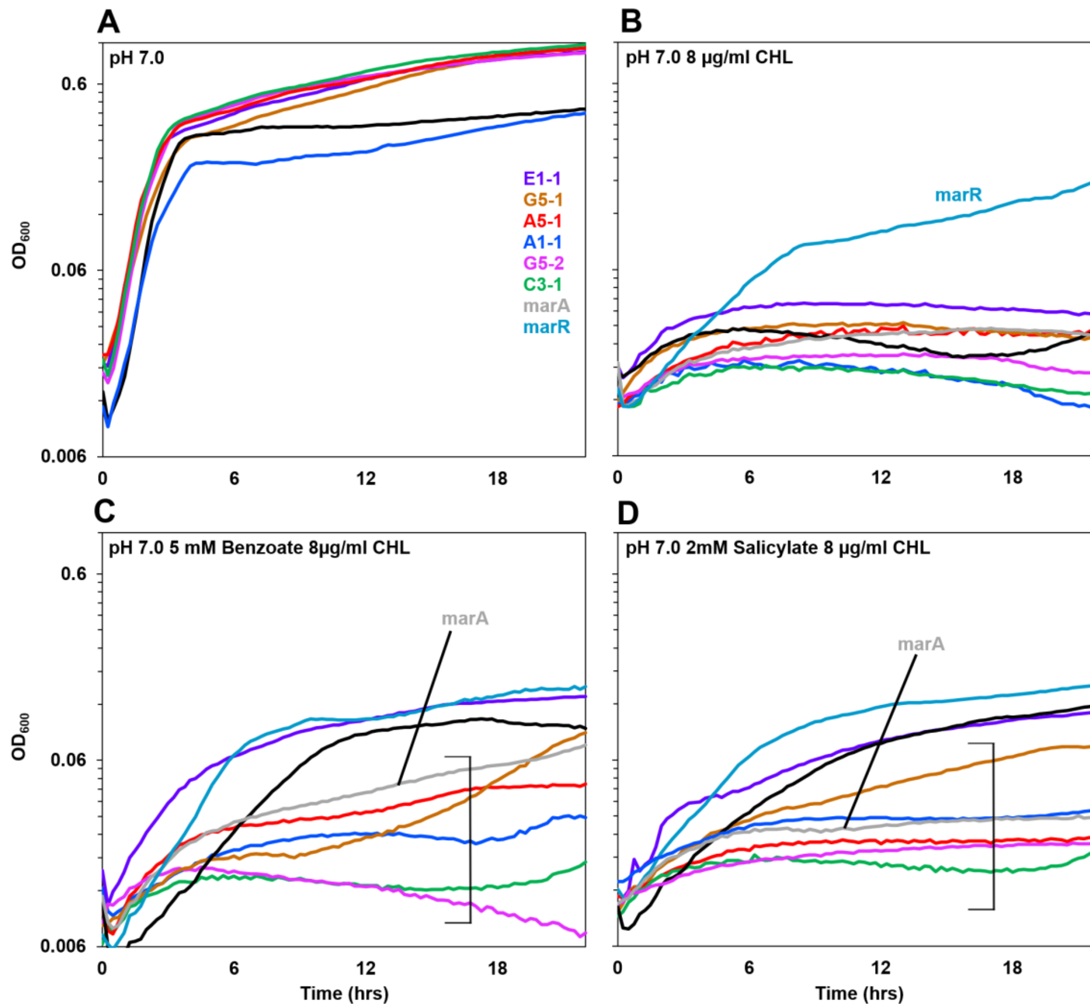

FIG 6 Benzoate-evolved strains are sensitive to chloramphenicol. Growth curves of benzoate-evolved strains and ancestor, compared to W3110 strains deleted for *marR* and for *marA*. Media contained LBK 100 mM MOPS pH 7.0 with (**A**) no supplements, (**B**) 8 µg/ml chloramphenicol, (**C**) 5 mM benzoate and 8 µg/ml chloramphenicol, (**D**) 2 mM salicylate and 8 µg/ml chloramphenicol. For each strain, a curve with median 16-h cell density is shown. Bracket indicates curves with cell density at16 hours that was lower than the cell density of ancestral strain W3110 (Friedman test; post-hoc Conover pairwise comparisons with Holm-Bonferroni adjusted p-values). For panels C and D, **Figure S3** shows all replicates of each strain plotted individually.

bioRxiv preprint doi: https://doi.org/10.1101/063271; this version posted October 22, 2016. The copyright holder for this preprint (which was not certified by peer review) is the author/funder. All rights reserved. No reuse allowed without permission.

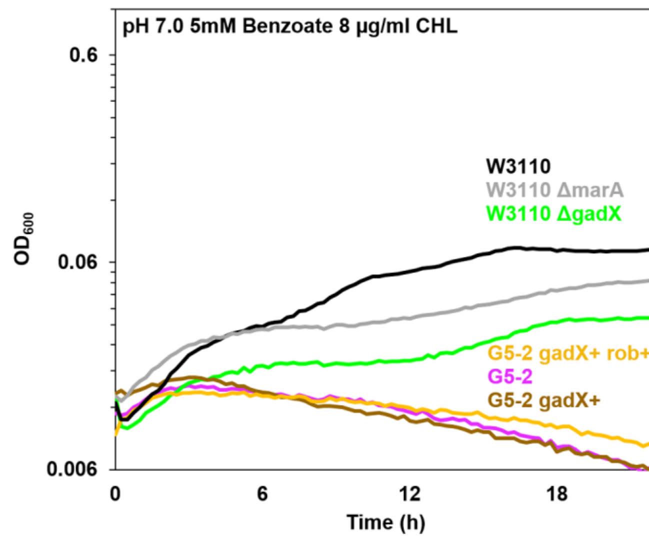

FIG 7 W3110 *gadX*::*kanR* shows sensitivity to chloramphenicol. Growth curves were conducted in LBK 100 mM PIPES pH 7.0 with 5 mM benzoate, 8µg/ml chloramphenicol, as for Figure 6. At 16 h, the *gadX*::*kanR* knockout and the *marA*::*kanR* strain both grew significantly less than strain W3110. The cell density of strain G5-2 showed no difference from those of G5-2 *gadX+* or of G5-2 *gadX+ rob+* (Friedman test; post-hoc Conover pairwise comparisons with Holm-Bonferroni adjusted p-values).